



EUROPEAN
COMMISSION

Community Research



ARCHER

Collaborative Project

Co-funded by the European Commission under the
Euratom Research and Training Programme on Nuclear Energy
within the Seventh Framework Programme

Grant Agreement Number: 269892

Start date: 01/02/2011 Duration: 48 Months

www.archer-project.eu



Application of the new COCOSYS model for recent HTR confinement strategies

Rebekka Gehr (RWTH)
Stephan Jühe (RWTH)

ARCHER project – Contract Number: 269892
 Advanced High-Temperature Reactors for Cogeneration of Heat and Electricity R&D
 EC Scientific Officer: Dr. Panagiotis Manolatos

Document title	Application of the new COCOSYS model for recent HTR confinement strategies
Author(s)	Rebekka Gehr (RWTH), Stephan Jühe (RWTH)
Number of pages	41
Document type	Deliverable
Work Package	WP23
Document number	D23.62 – revision 3
Issued by	RWTH
Date of completion	28/08/2014
Dissemination level	Restricted to the partners of the ARCHER project

Summary

This document contains a description and results of the efforts to simulate dust behaviour in the confinement of the HTR-Module 200 during a depressurisation accident. As initial events both a design basis accident as well as a beyond design basis accident have been analysed. For the former, the break of the Pressure Equalisation Line (PEL) has been chosen, which results in a nominal break area of $2 \times 37 \text{ cm}^2$. Due to flow losses from the reactor pressure vessel to the break location, the free rupture area has been adjusted to 20 cm^2 . The beyond design basis accident scenario is represented by a break in the pipe socket of the Fuel Feed Line (FFE), resulting in a break at the bottom of the reactor pressure vessel with a diameter of 350 mm and a free rupture area of 962 cm^2 respectively.

The simulations were carried out with the Containment Code System (COCOSYS), a zero-dimensional, so-called lumped parameter code.

Approval

Rev.	Short description	First author	WP Leader	SP leader	Coordinator
0	First issue	R. Gehr 28/08/2014	K. Verfondern (FZJ)	N. Kothz (TUV)	S. Knol (NRG)
1	First revision	R. Gehr 05/09/2014	K. Verfondern (FZJ)	N. Kothz (TUV)	S. Knol (NRG)
2	Second revision	R. Gehr 19/09/2014	K. Verfondern (FZJ)	N. Kothz (TUV)	S. Knol (NRG)
3	Third revision	R. Gehr 07/11/2014	K. Verfondern (FZJ)	N. Kothz (TUV)	S. Knol (NRG)

Distribution list

Name	Organisation	Comments
P. Manolatos	EC DG RTD	
All technical participants	ARCHER	
Steering Committee members	ARCHER	

Table of Contents

1	Nomenclature.....	4
2	Introduction	5
3	Choice of reference plant.....	6
	3.1 Plant description	6
	3.1.1 Primary circuit.....	6
	3.1.2 Confinement	7
	3.2 Description of break in the primary circuit	8
4	Choice of reference dust.....	10
	4.1 Dust amount	10
	4.2 Dust particle size and morphology	10
5	The COCOSYS code	14
	5.1 General description / Thermohydraulics.....	14
	5.2 Aerosol/Dust Models.....	14
	5.3 Improvements from COCOSYS V2.4 beta to V2.4.....	14
6	Modelling the depressurisation accident.....	16
	6.1 Confinement model.....	16
	6.1.1 General description of confinement nodalisation	16
	6.1.2 Basic reactor building model	17
	6.1.3 Refined reactor building model.....	18
	6.2 Dust injection	19
7	Analysis of Results.....	22
	7.1 Results for calculated dust behavior at PEL break.....	22
	7.2 Results for calculated dust behavior at FFE break.....	28
8	Potential consequences of COCOSYS' limitations.....	33
	8.1 Turbulent deposition	33
	8.2 Resuspension	34
	8.3 Variability of atmospheric material values	34
	8.4 Characteristic lengths for simulation of thermophoresis.....	34
	8.5 Input structure of injection tables	35
9	Summary and Perspective.....	36
10	Literature	38
11	Annexes	40
	11.1 Annex 1: Document approval by beneficiaries' internal QA	41

1 Nomenclature

Abbreviation	Meaning
AFP	Aerosol Fission Product Behavior (module for COCOSYS)
ASTEC	Accident Source Term Evaluation Code
AVR	Arbeitsgemeinschaft Versuchsreaktor
CCI	Core Concrete Interaction (module for COCOSYS)
COCOSYS	Containment Code System
DBA	Design Basis Accident
DIREKT	Thermal-Fluid code with direct solver
FFE	Pipe for fuel feed equipment
FIPLOC	Containment simulation program
GRS	Gesellschaft für Anlagen- und Reaktorsicherheit
HTR	High Temperature Reactor
INST	Incompressible transient momentum equation (model for mass flow calculation in COCOSYS)
KLAK	Kleine Absorber Kugeln (small absorber spheres)
KOAX	Coaxial duct
LOCA	Loss Of Coolant Accident
ORIFICE	Orifice flow model (model for mass flow calculation in COCOSYS)
PEL	Pressure Equalization Line
RALOC	Radiolysis and Local Gas Concentration (forerunner of COCOSYS)
SPECTRA	Sophisticated Plant Evaluation Code for Thermal Hydraulic Response Assessment
STAR	Staubtransport, -ablagerung und -resuspension (dust transport, deposition and resuspension)
THTR	Thorium High Temperature Reactor
THY	Thermal Hydraulics (module for COCOSYS)

<u>Symbol</u>	<u>Unit</u>	<u>Meaning</u>
d	m	Particle diameter
q_0	$\frac{1}{m}$	Distribution density: number weighted
q_3	$\frac{1}{m}$	Distribution density: mass weighted

R_{red}	-	adhesive reduction due to surface roughness
\dot{q}''	$\frac{W}{m^2}$	Heat flux
Sc	-	Schmidt-number
∇T	$\frac{K}{m}$	Temperature gradient
T_W	K	Wall temperature
T_{fl}	K	Fluid temperature
u_τ	$\frac{m}{s}$	Friction velocity
$v_{dep,turb}$	$\frac{m}{s}$	Deposition velocity for turbulent deposition
α	$\frac{W}{m^2 K}$	Heat transfer coefficient
ρ_{fl}	$\frac{kg}{m^3}$	Fluid density
λ_{fl}	$\frac{W}{m K}$	Thermal conductivity of the fluid
η	$\frac{kg}{m s}$	Dynamic viscosity
σ_g	-	geometric standard deviation of the adhesive forces
τ	s	Relaxation time
τ^+	-	Dimensionless relaxation time

2 Introduction

Carbonaceous dust is formed during normal operation of HTR due to several mechanisms. Because dust interacts with fission- and activation products, it is a significant activity carrier. Dust is deposited on primary circuit surfaces, from which it can be resuspended during depressurisation accidents. Current HTR-concepts will not be provided with a gas tight containment, but with a “filtered/vented confinement” from which gases will be released into the atmosphere in case of a significant break in the primary circuit. Thus, certain amounts of dust will exit through the breach of the primary circuit and eventually from the confinement into the environment. The analysis of that source term chain for dust has been considered as a major safety issue for HTR [INL11a], [JÜH12].

Within the last deliverable D23.61 [Jüh12a], the status of the work undertaken to simulate dust behaviour in the confinement of a selected HTR reference plant was presented. This deliverable includes the results of the repeated simulation with the new CCOCOSYS version (May 2013) as well as new results from the simulation of another break scenario.

3 Choice of reference plant

Because dust behaviour depends on plant geometry and fluid dynamic conditions, its analysis cannot be performed for HTR in general, but only with respect to a specific reference plant.

Due to its technical maturity, its still existing relevance for current HTR projects and the availability of detailed information on plant design, the HTR-Module-200 in 2-Block layout was selected as the reference plant for the analysis presented here.

A comprehensive plant description is given in [INL11b] and partly in [REU84].

3.1 Plant description

3.1.1 Primary circuit

A large fraction of the primary circuit volume of 460 m^3 takes part in the normal operation helium circulation. A simplified illustration of the gas flows is given in figure 1.

Passing through the pebble bed (1), the helium is heated to a medium temperature of 700 °C . Then it flows through bores in the bottom reflector (2) and mixing chambers into the torus-shaped hot gas collector (3). From there, it is led through the inner tube of the coaxial duct (4) into the steam generator (5). Heat is transferred to the steam generator tubes, cooling the gas to 250 °C . From there, it flows to the blower (6), which generates the differential pressure of $0,15\text{ MPa}$ necessary to maintain helium circulation against the flow resistance. Through the outer part of the coaxial duct the gas gets to the annulus (7) between reactor pressure vessel and core barrel. After passing the bottom of the reactor pressure vessel, the helium flows through the side reflector (8), a small cavity above the top reflector (9) and through bores into the space above the pebble bed.

Additionally, the primary circuit features volumes with stagnating helium. These are especially the gas plenum in the upper calotte of the reactor pressure vessel (a) and the cavity between top reflector and thermal shield (b), but also the annuli between reactor pressure vessel and core barrel (c) as well as core barrel and side reflector (d) and the structures (e) containing the discharge vessels of the KLAK system.

Through the outer pressure compensation line, the outer annulus is connected with the blower-buffer. Furthermore, the gas plenum in the upper calotte of the reactor pressure vessel is connected with the cold gas-filled region via the inner pressure compensation line, which is closed during normal operation by a rupture disc and allows for the gas to exit during a depressurisation accident with the intention of preventing destructive pressure differences over the core structures.

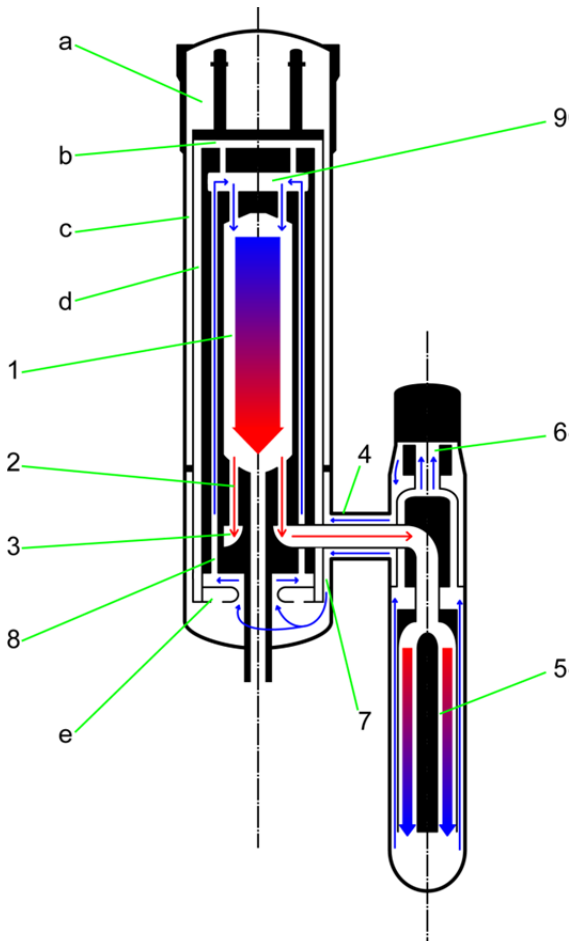


Figure 3-1 : Helium flow in the HTR-Module

3.1.2 Confinement

A schematic of the plant geometry with respect to the pressure relief path is shown in Figure 3-2. The reactor and steam generator cavity surrounding the primary circuit are connected with a relief opening to the fuel handling room, which in turn is connected with the rooms of the module block on the $-9,55\text{ m}$ level. Up to the $+9,50\text{ m}$ level gas can flow freely within the rooms of the module block. The upper part is connected to a pressure relief duct, which is closed by a rupture disk during normal operation and leads into the reactor building at approx. $+28\text{ m}$. Because of relief openings at $+31,9\text{ m}$, leading to the chimney, a significant part of the volume of the reactor building is not part of the depressurisation flow path. On the $\pm 0\text{ m}$ level, a door opening at overpressure connects the reactor building to the rooms of the other module block as well as two stairwells.

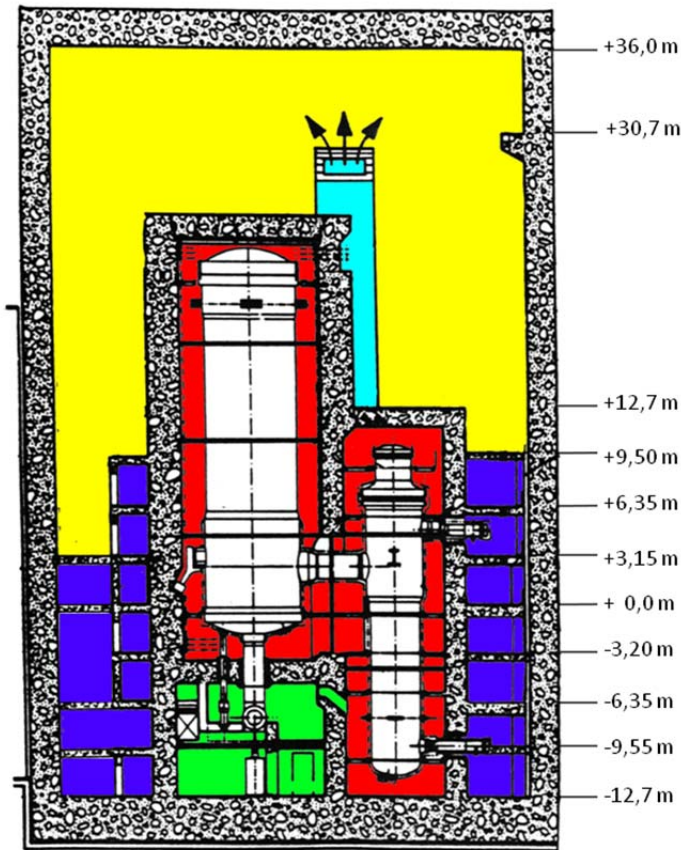


Figure 3-2: Schematic illustration of the volumes relevant for depressurisation for the HTR-Module (modified from [INT679])

3.2 Description of break in the primary circuit

The location of the leaks assumed in [JÜH11] for the HTR-Module are shown in Figure 3-3. The components designated by the abbreviations are the Pressure Equalization Line (PEL), pipe for Fuel Feed Equipment (FFE) and the Coaxial Duct (KOAX).

A break of the PEL has been considered a design basis accident (DBA) for the HTR-Module, while breaks of FFE and KOAX have been excluded as DBA. Nonetheless, as beyond design basis accidents, their analysis is still of interest for nuclear safety research.

In the last Deliverable D23.61 [JÜH12a], it was argued that only PEL has to be analysed, since results of PEL and FFE differ only quantitatively; while for KOAX, no meaningful analysis of dust behaviour is possible because of the severe destruction caused by such a break [JÜH11]. Still, for this deliverable both PEL and FFE were simulated, confirming previous assumptions. The quantities of released dust into the confinement/environment differ significantly, but the progress of relative dust release remains almost the same.

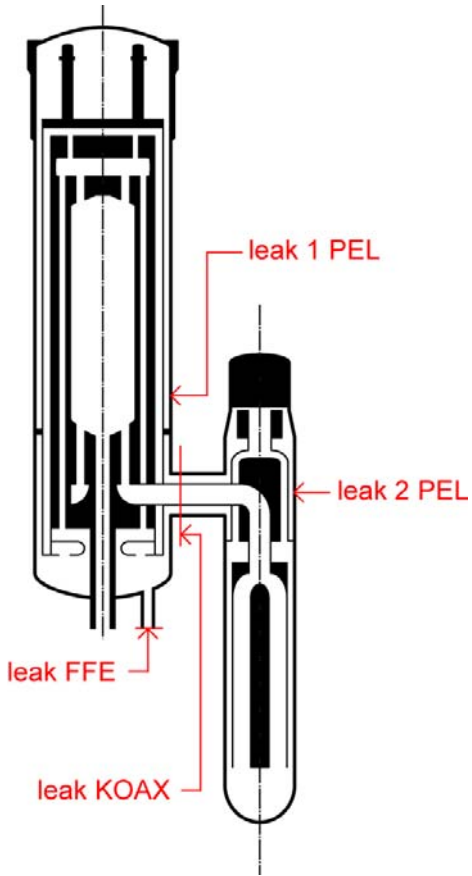


Figure 3-3: Locations of possible leaks

4 Choice of reference dust

In order to be able to make quantitative predictions about the dust bound source term for the HTR-Module, existing knowledge about dust in pebble bed HTR has been refined.

4.1 Dust amount

When transferring experience with dust produced in the AVR and THTR reactors (which however is afflicted with uncertainties) to other plants, than e.g. thermal power or the number of fuel element cycles can be used as a scaling factor. Additionally, an experimentally determined production rate of 10 mg dust per fuel handling is stated for the HTR-Module [IAE97]. Altogether, there is no evidence contradicting the original prediction of an overall dust production of 500 – 1000 kg for the HTR-Module within 32 full-load years [INT87/88], [SCE88]. For the scope of the analysis presented in this deliverable, the upper limit of 1000 kg from [IAE97] has been premised, which is consistent with other works [JÜH11], [JÜH12].

4.2 Dust particle size and morphology

For all aspects of dust behaviour, size distribution of dust particles are of great importance. The dimensions of non-spherical particles can be determined and described by various methods, yielding results that cannot be directly compared.

Unfortunately, most of the sources cited here do not take that into account – the characterization of dust is performed just by the particle diameter without further information. Only in [FAC08b], the circle diameter of an identical projection area as the particle is given; a systematic analysis of particle morphology is not documented, either.

Due to the lack of substantiated information regarding the morphology of HTR-typical dust particles, within the scope of this work particles are assumed to be massive and spherical. This simplification was also used by [FON09].

A theoretical prognosis of the particle sizes produced by abrasion is not possible at the present state of knowledge. Anyway, there is no definite answer to the question about the dominant production mechanism for carbonaceous dust, and the results of experiments for dust production via abrasion and chemical reactions are not assured to reflect actual HTR conditions. Consequently, the determination of the particle size spectrum solely depends on HTR operation experience.

Three sources were utilized for the determination of particle size distribution:

1. AVR dust analysed 20 years after shutdown [FAC08a]
2. AVR dust analysed during reactor operation [GOT90]
3. THTR dust [OET89]

The corresponding size distributions are shown in Figure 4-1 to Figure 4-3. Due to counting statistics, the data for mass weighted distributions for the AVR dust are to be interpreted with care, because of the very low frequency of big particles in the originally number weighted distribution given in the sources.

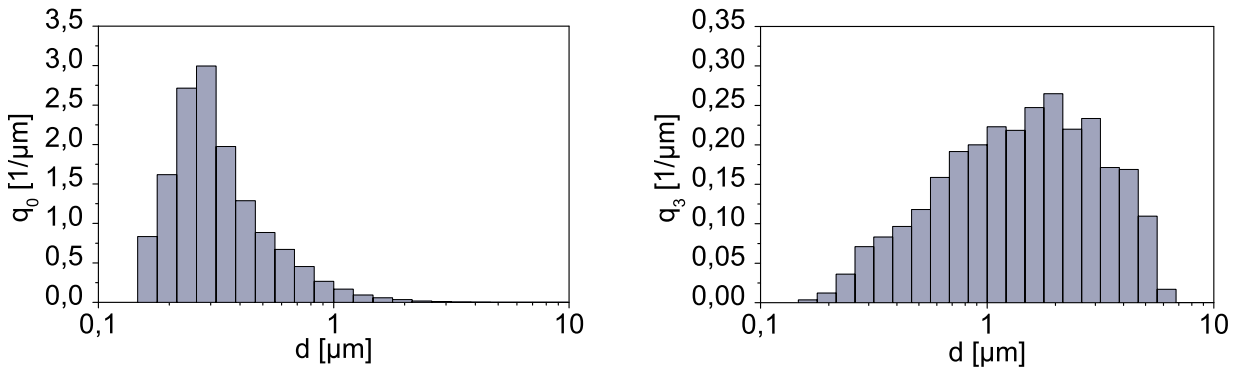


Figure 4-1: Particle size distribution density for AVR dust according to [FAC08a]/[FAC08b]: Number weighted (left) and mass weighted (right)

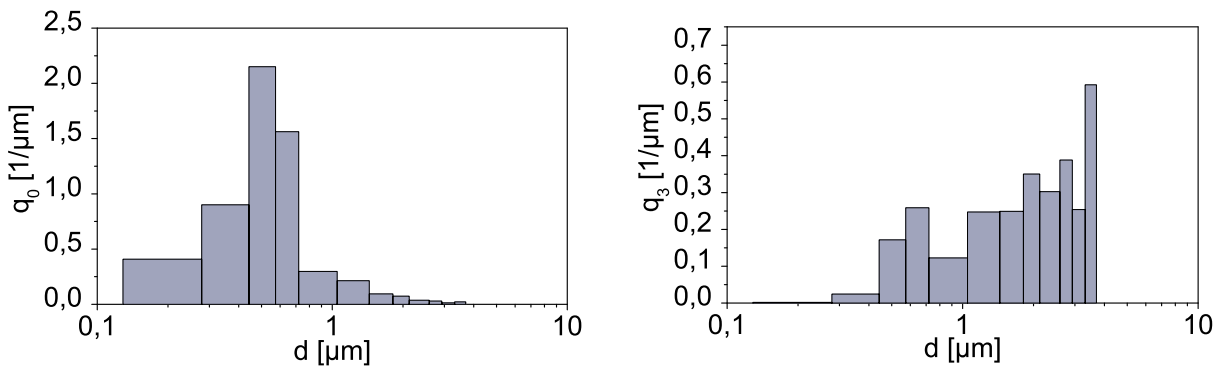


Figure 4-2: Particle size distribution for AVR dust according to [GOT90]: Number weighted (left) and mass weighted (right)

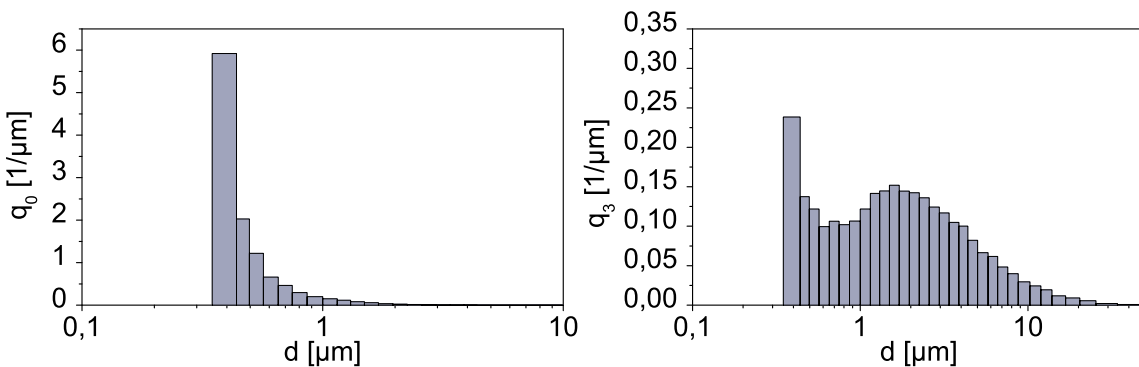


Figure 4-3: Particle size distribution of THTR dust according to [OET89]: Number weighted (left) and mass weighted (right)

Since it is not possible to make an universal statement, whether an under- or overestimation of particle size can be considered conservative for depressurisation events, the data from the three sources presented above are used to define the particle size distribution scenarios S1 to S3.

For the use in COCOSYS, the number of particle size classes is limited to 20; except for absolute upper and lower limit, the discretization is determined internally.

The characterisation of HTR dust for all 3 scenarios is given in Table 1 and Figure 4-4.

Table 1: Dust particle size distributions

#	Size class			Fraction S1 AVR after shutdown [mass %]	Fraction S2 AVR during operation [mass %]	Fraction S3 THTR [mass %]
	d^{min} [μm]	d^{max} [μm]	d^{lm} [μm]			
1	0.1000	0.1413	0.1189	0.0000	0.0022	0.0000
2	0.1413	0.1995	0.1679	0.0372	0.0101	0.0000
3	0.1995	0.2818	0.2371	0.3318	0.0217	0.0000
4	0.2818	0.3981	0.3350	0.9453	0.2830	1.2012
5	0.3981	0.5623	0.4732	1.7963	2.1713	2.5595
6	0.5623	0.7943	0.6683	4.0525	4.8836	2.3936
7	0.7943	1.1220	0.9441	6.8056	4.9169	3.6449
8	1.1220	1.5849	1.3335	10.4858	11.4719	6.6520
9	1.5849	2.2387	1.8836	16.5958	20.0589	9.4792
10	2.2387	3.1623	2.6607	21.0460	29.6483	11.7314
11	3.1623	4.4668	3.7584	22.1873	26.5321	13.5132
12	4.4668	6.3096	5.3088	14.8646	0.0000	12.8436
13	6.3096	8.9125	7.4989	0.8517	0.0000	11.6634
14	8.9125	12.5893	10.5925	0.0000	0.0000	9.3483
15	12.5893	17.7828	14.9624	0.0000	0.0000	6.8651
16	17.7828	25.1189	21.1349	0.0000	0.0000	4.9354
17	25.1189	35.4813	29.8538	0.0000	0.0000	2.0808
18	35.4813	50.1187	42.1697	0.0000	0.0000	1.0885
19	50.1187	70.7946	59.5662	0.0000	0.0000	0.0000
20	70.7946	100.0000	84.1395	0.0000	0.0000	0.0000

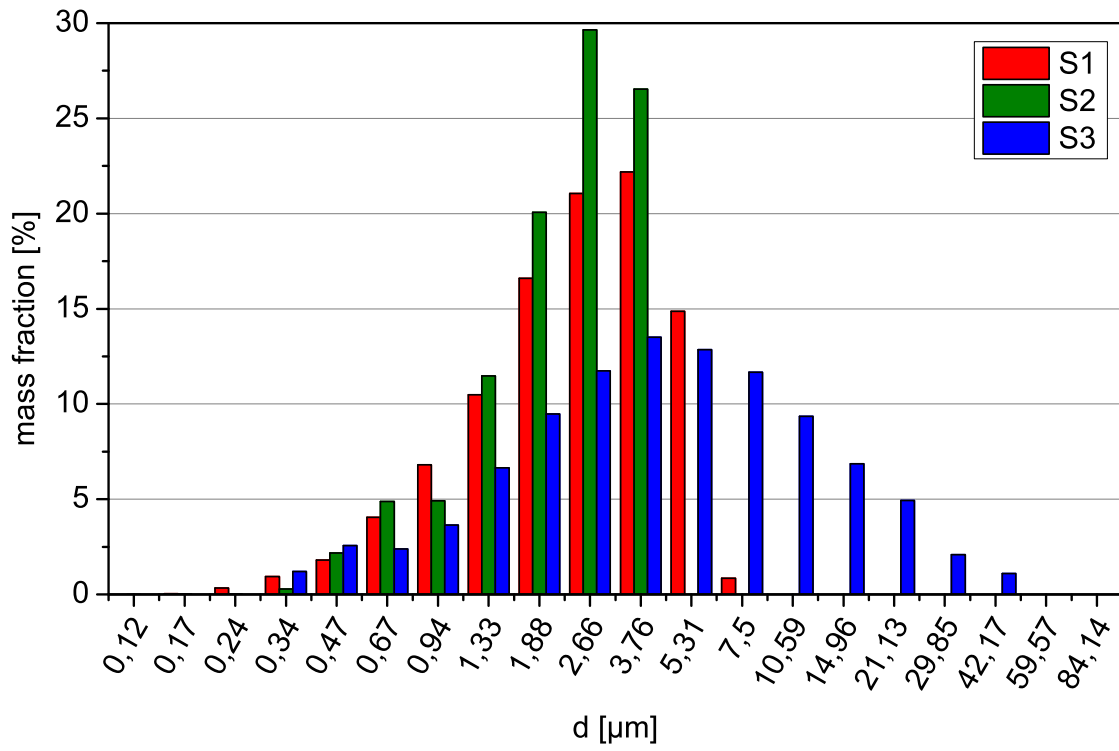


Figure 4-4: Dust particle size distributions

5 The COCOSYS code

Based on several codes, amongst others RALOC and FIPLOC, the German GRS develops the containment code system COCOSYS [ALL08]. The goal is to be able to simulate all containment phenomena following design basis accidents as well as severe accidents of light water reactors through mechanistic models [KLE10].

5.1 General description / Thermohydraulics

The principal modules of COCOSYS are THY (Thermal Hydraulic) and AFP (Aerosol and Fission Products); an additional module CCI (Corium Concrete Interaction) is not needed for most applications.

As a “lumped parameter code”, COCOSYS requires the geometry to be divided into several zero-dimensional zones (depending on the application 20-200), which thermohydraulically interact via junctions. The zones can be subdivided into several zone parts, which is relevant only for scenarios involving liquid plus gaseous fluids and therefore negligible for depressurisation accidents of HTR.

Flow resistance occurs at the junctions connecting the individual zones, thus together with the driving forces (pressure differences) determining the gas flow between the volumes. Additionally, models for components like rupture disks or flaps are included into the junction calculation.

Heat transfer to walls and through walls between different zones can be simulated through the modelling of heat conducting materials in a feature called “structures”.

The thermohydraulic influence of different accident management measures can be simulated in COCOSYS, too; due to their irrelevance for HTR depressurisations, their description is omitted here.

5.2 Aerosol/Dust Models

For the simulation of aerosol and fission product behaviour, several mechanisms are taken into account and only the ones relevant for the task at hand are described here:

Aerosol-related calculations are performed for each zone. The particle size range is discretized into several (up to 20) particle size classes. Particles can be deposited on walls; the mechanisms modelled in COCOSYS are:

- Sedimentation
- Diffusive deposition
- Thermophoresis
- Diffusiophoresis

Additionally, agglomeration of particles is considered. Resuspension from dry surfaces can be calculated according to the Fromentin model; its implementation is, however, only applicable to events like hydrogen deflagrations or steam explosions.

5.3 Improvements from COCOSYS V2.4 beta to V2.4

There have been several changes from COCOSYS' beta version to the released version: The released version includes a new heat conductivity model for structures, CO1, for free/forced convection as well as condensation/evaporation. Furthermore, user-defined parameters from the input deck have been limited to minimal/maximal values, since experience showed that user definition resulted in distortion of results. E.g. too thick layers in nodalisation of structures, especially structures to the environment, resulted in a huge overestimation of structure's heat sink potential [STE82], [ERD91].

So all changes in COCOSYS have a high impact, when simulating relatively long-lived phenomena, like heat transfer from/to structures with a steam-filled atmosphere or building/evaporation of water pools in the containment over a long period.

Another relevant change is an error correction (“bug fixing”) on the temperature calculation for thermophoresis. Due to this bug, the maximum temperature difference between the boundary layer for

thermophoresis and the atmosphere was predicted too low. Likewise the amount of particle deposition based on thermophoresis was also underestimated.

As the discussion of the results of the calculations performed in the following chapters will show, for dust behaviour after a PEL/FFE break these changes in COCOSYS have a very limited relevance, due to the fact that blow-down phase of depressurisation accidents as well as the duration of the simulation (500 s) is too short and results are dominated by short-lived phenomena, especially the high fluid flow velocities immediately after the depressurisation accident occurs.

6 Modelling the depressurisation accident

Due to the scope of this deliverable, the focus of the presentation of the work performed is on the modelling of the depressurisation accident in COCOSYS. The COCOSYS calculations require injection tables for both the gas and the dust entering the confinement through the breach of the primary circuit. Thus, a complete simulation of fluid dynamics and dust behaviour in the primary circuit is a prerequisite to any subsequent work. A short overview of the work preceding the COCOSYS-modelling taken from [JÜH12] is given here for better understanding.

While for the simulation of the fluid dynamics an enhanced version of the DIREKT code, developed at the Forschungszentrum Jülich, was used, for dust behaviour, a comprehensive code STAR (Source Term due to Aerosol Resuspension) was developed and coupled with DIREKT.

The STAR code incorporates correlations for deposition, surface interaction, resuspension and transport of dust.

Mechanisms identified as relevant for dust deposition in the not stagnating volumes of the primary circuit are thermophoresis, diffusion, impaction and turbulent deposition. Thermophoresis is calculated according to the Talbot-equation [TAL80], [AHM98] and turbulent deposition with the correlation according to [WOO81]. Diffusive deposition and impaction at bends/deflection plates is calculated with the respective correlations given by [HIN99]. For impaction in the pebble bed and on the steam generator pipe bundle the correlations from [GOR82] and [HER07] are used, respectively. For turbulent flow turbulent deposition is calculated for these geometries according to [WOO81] too, while for laminar flow the correlations used are taken from filter efficiency calculations [ING81], [LÖF88].

The average adhesive force of dust particles on the surface is calculated with the Derjaguin-Muller-Toporov-(DMT) Model [CAR05]. The degree of variation of the adhesive forces is characterized by the geometric standard deviation σ_g . The adhesive reduction due to surface roughness (for definition: [REE01]) is incorporated through a particle-size-independent reduction factor R_{red} . Since dust deposits in AVR were observed as hard and crust-like [FAC08a], surface-bound dust was modelled as the original primary particles without any formation of resuspendable clusters. Multi-layer effects were taken into account to the extent that only the uppermost part of the deposit, expressed through the free-fraction θ , is allowed to interact with the fluid.

For the simulation of dust resuspension the quasi-static Rock'n Roll model [REE01] was selected because of its sound theoretical foundation and simplicity of application. Its implementation is similar to the SPECTRA code [STE10a]; however, no parts of the resuspension rate equation were left out for simplification reasons. The compliance with the model's limit of validity (notably, turbulent flow conditions and the validity limits of the aerodynamic force correlations) is monitored by the code. Dust transport was calculated considering the interaction of deposition, resuspension and convective transport, the latter being imposed by the mass flows calculated by the thermal hydraulics code DIREKT.

A more detailed description of the work performed for the development and validation of STAR and the modelling of the primary circuit of the HTR-Module for the calculation of normal operation and depressurisation events is given in [JÜH11], [JÜH12].

It should be noted that the reason "simplicity of application" for selecting the quasi-static Rock'n Roll model is not simply a matter of convenience, rather than a reference to its advantages of being dependent on very few parameters to be determined and of requiring only a modest numerical effort. The top-layer thickness for the calculation of θ was found to have little effect on integral resuspension; typically, a value of $1 \mu\text{m}$, representing the smaller particles of the dust spectrum, was used.

6.1 Confinement model

6.1.1 General description of confinement nodalisation

In [JÜH12a], the confinement was nodalised like in figure 6-1 by using manufacturer's information of the HTR-Module. The figure shows a compacted view, for which the zones of the reactor building and the

stairwells were merged. It is shown here again, because the changes in nodalisation only apply for the reactor building (RG) and therefore, figure 6-1 is still a valid overview of the nodalisation.

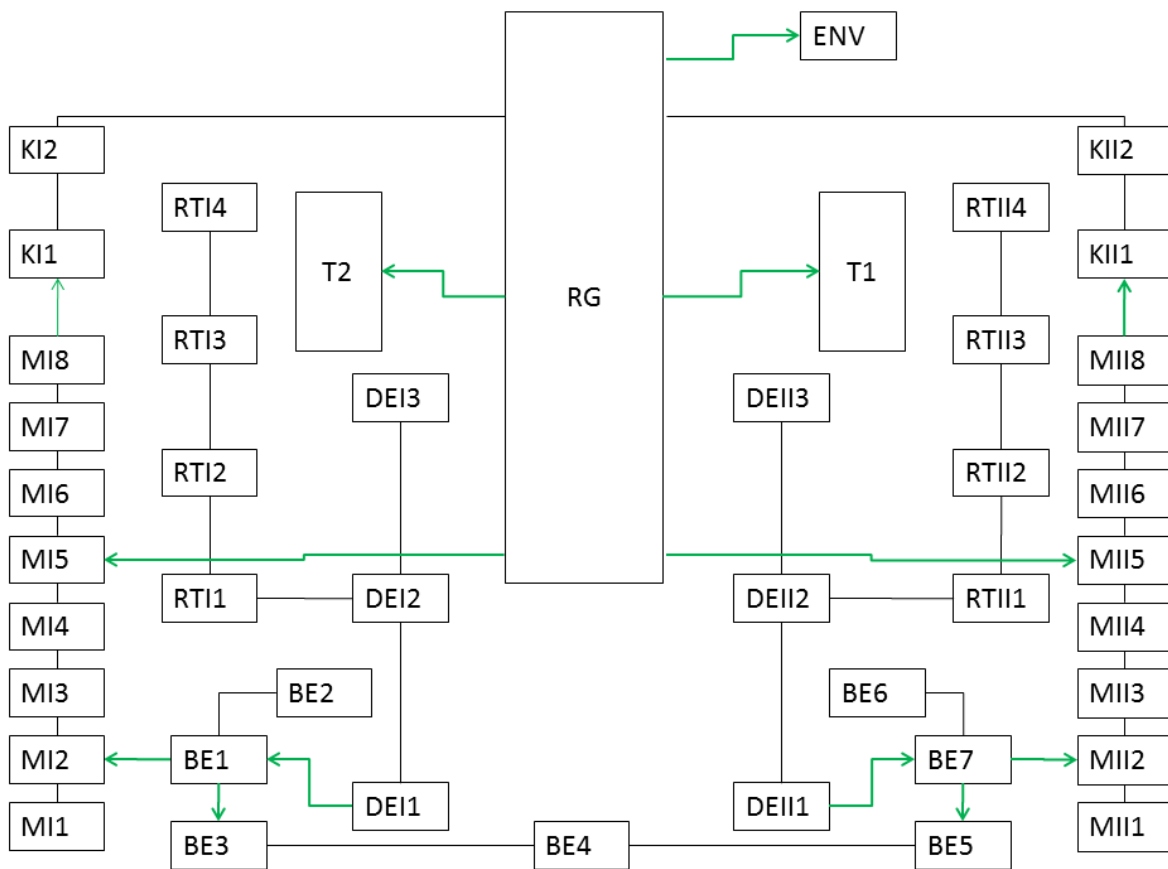


Figure 6-1: COCOSYS nodalisation of the rooms of the HTR-Module (compacted view, see Table 2 for explanation)

6.1.2 Basic reactor building model

In following Figure 6-2 and Figure 6-3 one can see an overview of the general configuration of the zones comprising the reactor building. Here, yellow stands for the reactor floor, green for the steam generator floor, red for the erection shaft and blue for the main transport route. For the sake of clarity, the connection of the zones through atmospheric junctions is illustrated merely by positioning them adjacently.

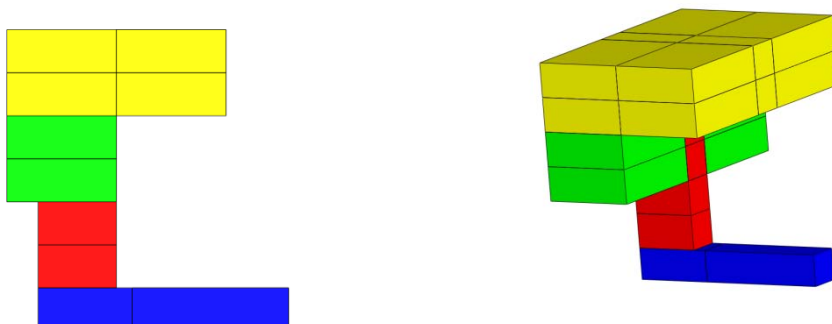


Figure 6-2: COCOSYS nodalisation of the reactor building (old nodalisation)

A breakdown of the abbreviations used is given in Table 2. In the nodalisation scheme, atmospheric junctions are indicated with a simple black line, while a green arrow (indicating the opening direction) stands for a rupture disk- or flap junction.

Table 2: Explanation of the zone designations for the COCOSYS nodalisation

First digit		Second digit		Third digit
Abbrev.	Meaning	I	Block 1	Running number
RT	Reactor cell	II	Block 2	
DE	Steam generator cess			
BE	Fuel element handling room			
M	Rooms of module block			
K	Pressure relief duct			
T	Stairwell			
RG	Reactor building			
ENV	Environment			

Due to the significant differential pressures occurring during depressurisation, for all junctions with rupture disks or flaps the ORIFICE-Model, in all other cases the INST-Model is used¹. Considering the short simulation time of 500 seconds, heat conducting structures representing the concrete surfaces were defined for each zone bordering to a wall area, but no heat transfer between the zones through these structures was introduced.

6.1.3 Refined reactor building model

One identified potential for improvement, pointed out in [JÜH12a], was the simulation of an accident scenario using a more detailed nodalisation and modelling of (atmospheric) plume structures. Plume nodalisations are advantageous when simulating phenomena that depend on temperature and density differences; e.g. buoyancy driven phenomena, like H₂ agglomeration under a ceiling or steam/air convection loops through a containment after a LOCA incident in a light water reactor [BRO13]. Even if buoyancy driven phenomena proceed physically slowly – in comparison to others – those processes were predicted as too slow by COCOSYS. Using the plume nodalisation enhances (accelerates) processes in simulation, so that there is a better conformity between simulated and experimental data.

In case of a PEL all events run very fast: the leak impulse into the confinement immediately after the appearance of a leak as well as the simulation time of only 500 s. Plume nodalisation accordingly turns out to be without any impact [BRO13].

Hence, only a refined grid was tested, which is shown in Figure 6-3.

¹ ORIFICE and INST are the names for COCOSYS-internal simulation models for mass transport via flow paths.

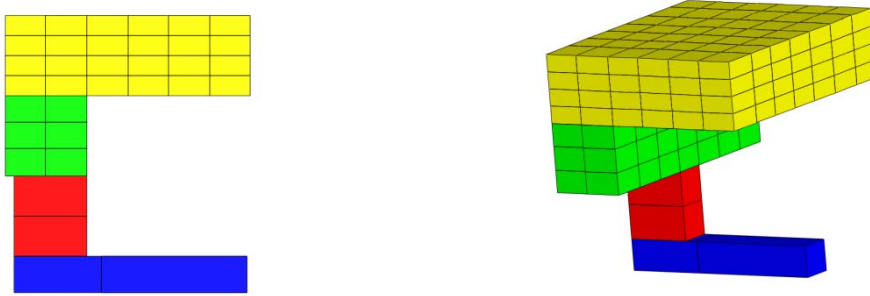


Figure 6-3: COCOSYS nodalisation of the reactor building (new nodalisation)

This close-meshed nodalisation may not have benefits for buoyancy processes, but it does improve results by reducing numerically induced diffusion [BUR13]. Irrespective of the used code the results are influenced by the user through the chosen nodalisation. As a benchmark, the Courant-Friedrichs-Lewy condition (abbreviated CFL condition or in one-dimensional cases also referred to as CFL number or Courant number) is used. The Courant number describes the transport velocity of the state of one cell (e.g. mass or particle concentration in a cell) to the next cell, regarding the difference between the centres of the cells:

$$C = \frac{u \cdot dt}{dz}$$

Where u is the velocity, dt the size of the time step and dz the difference between centres of adjacent cells.

The simplification in numerical equations (differences instead of differentials) results in $C < 1$, respectively in diffusion and artificially (numerically) expanded particle concentration gradients.

It is a general practice to reduce the cell size to gain an improvement in accuracy. However, this method works at the expense of calculation time. So it depends on user's skills to find a proper balance between cell size and simulation time. If repeated simulations with a finer grid show similar behaviour than previous ones, a adequate grid had already been chosen. So simulations with refined grids either confirm the results obtained with the previous nodalisation or improve accuracy.

This applies especially for LP-codes which can not simulate fluid fronts so that the atmospheric mixture inside one control volume is homogenous.

6.2 Dust injection

A crucial issue for the simulation of dust behaviour in the primary circuit is the determination of the parameters characterizing the adhesive forces, σ_g and R_{red} . Since for graphite dust, the experimental results from [REE01] could be reproduced with $R_{red} = 15$, $\sigma_g = 5.0$, these values were considered the expected case. Additionally, a variation study was performed from $R_{red} = 7.5 \dots 200$ and $\sigma_g = 2.0 \dots 5.0$.

The results for the integral dust mass exiting the primary circuits through the leak in the Pressure Equalization Line are shown in

Figure 6-4 a-c for dust particle size distribution scenarios S1 to S3, and Figure 6-5 for break of the fuel feed line, respectively.

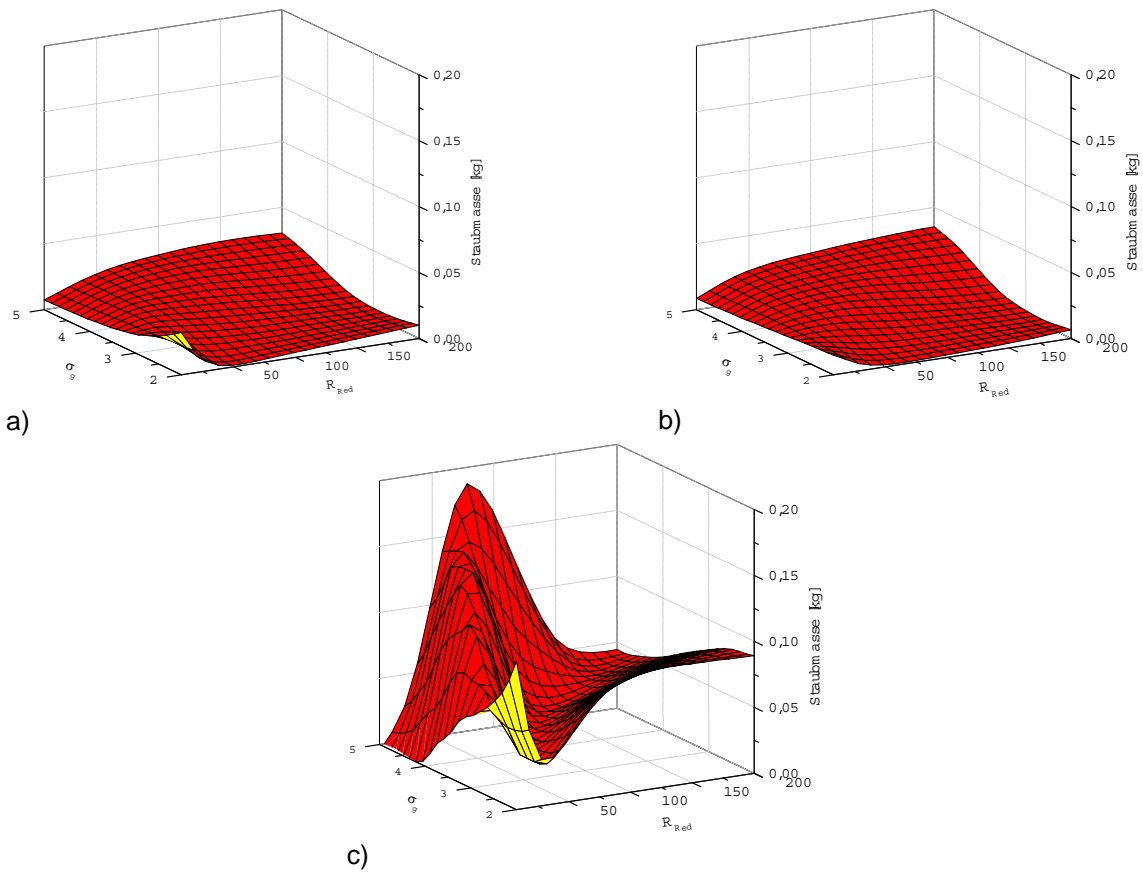
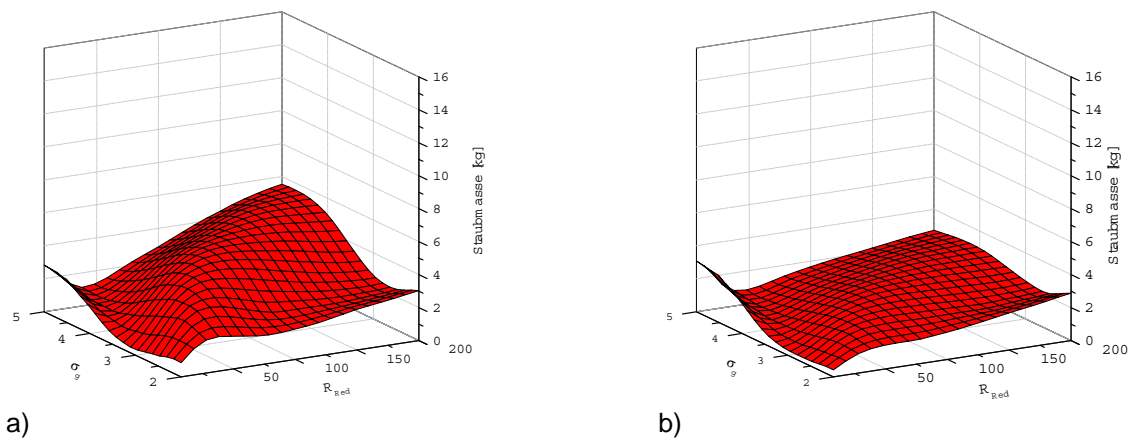
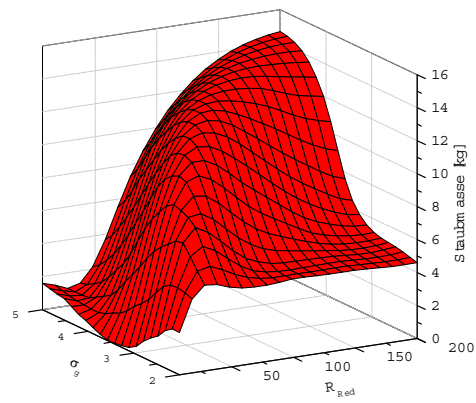


Figure 6-4: Dust release at PEL break as a function of adhesive force parameters for
 a) Dust particle size distribution scenario S1
 b) Dust particle size distribution scenario S2
 c) Dust particle size distribution scenario S3





c)

Figure 6-5: Dust release at FFE break as a function of adhesive force parameters for

- Dust particle size distribution scenario S1
- Dust particle size distribution scenario S2
- Dust particle size distribution scenario S3

The results show that there is no unambiguous correlation between adhesive forces and dust release.

Since the focus of this deliverable is the modelling of dust behaviour with COCOSYS and not an uncertainty analysis for the dust source term into the environment, only the dust injection into the confinement for the expected case ($R_{red} = 15$, $\sigma_g = 5.0$) is considered in the following analysis. The significant differences of the dust mass released from the breach of the primary circuit into adjacent rooms of the building for alternations of the adhesive model parameters do point out that validation of the correct values of those parameters for actual HTR operating conditions is an important goal for further research efforts.

7 Analysis of Results

The results presented in chapter 4.1 of [JÜH12a] were obtained with the then available Version 2.4 beta of COCOSYS, whereas newer simulations for this deliverable were carried out by the released Version 2.4. In order to test the potential influence of using different COCOSYS versions, input decks used to generate results presented in last deliverable got slightly modified to make them runnable in COCOSYS V2.4: the only modification is the amount of temperature nodes in structures, since V2.4 requires min/max values which did not exist in the beta version. Results of V2.4-reruns show an almost perfect conformity regarding thermal hydraulics and the dust released into the environment with ones of beta version. Therefore any influences of different COCOSYS versions can be neglected.

For the depressurisation of the primary circuit, one should be aware that COCOSYS is a code for containment phenomena and hence does not have an explicit simulation model to simulate the primary circuit of a HTR. As a consequence, mass flow rates, temperature and pressure of helium release plus dust release into the containment are determined by using the codes DIREKT and STAR [JÜH11]. These so obtained values are used in COCOSYS as external sources/injections into the COCOSYS control volume that is located at the postulated leak position.

For the discussion of the results from both break scenarios, the focus is purely on the released dust source term, not on the radiological load the dust may carry. The correlation between dust and radiological source term has been a subject in the past [INT561] and is still a current subject in research [JÜH11] as well as a fundamental radiological source term in high temperature reactors.

7.1 Results for calculated dust behavior at PEL break

In the design of the HTR-Module-200, the PEL is a DN 65 pipe [INL11a], [INL11b] so that the resulting rupture area is 37 cm². Contrary to other break scenarios, where the pipe connects the primary circuit with an auxiliary system, the break of the PEL at the steam generator is a break inside of the primary circuit. For this reason, the primary circuit depressurisation occurs on both sides of the break, doubling the rupture area to 2 x 37 cm². The calculation of pressure losses in long piping at almost sonic velocity is not covered by the models implemented in DIREKT. Additionally, the design of the PEL is not documented in sufficient detail in the plant description to allow an integration into the primary circuit model. Therefore, the cross section of the break is adjusted to 20 cm² to cover the pressure losses in the piping. By this approach, consistency with the calculations from [INT679] for the break at the RPV side is accomplished. For the steam generator side of the break, the calculated mass flow rates match the results from [INT679] very well without modification.

The effect of the confinement for dust retention at the break of the Pressure Equalization Line and the expected case of dust adhesive force parameters is summarized in Table 3

Table 3: Confinement dust balance for dust particle size distribution scenarios S1 - S3

	S1	S2	S3
Total dust mass injected into confinement	10.2 g	11.9 g	6.4 g
Total dust mass released into ENV	3.5 g	4.1 g	2.1 g
Released fraction	34 %	35 %	33 %

Generally, it can be stated that while some of the dust is retained in the confinement, a significant amount still escapes into the environment. Content of Table 3 is also valid for the repeated simulation with the released code version, COCOSYS V2.4. Numbers of dust mass do only change after the third decimal place. As an example the influence of the deposition of dust on the released fraction is illustrated in Figure 7-1 for particle size distribution scenario S3. In that graph, the relative dust mass released into ENV stands for the ratio of the mass released up to that simulation time into the environment and the respective value at the end of the depressurisation. The fraction of the deposited dust mass refers to the cumulated dust mass injected into the confinement at the corresponding time.

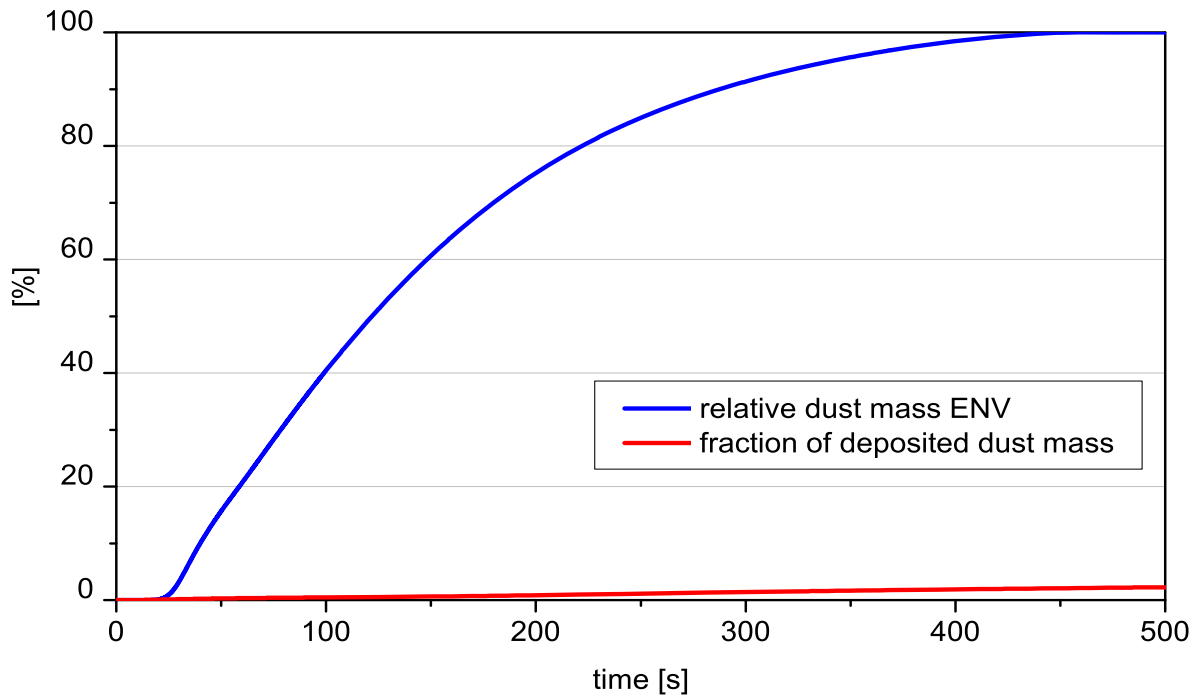


Figure 7-1: Relative dust release and deposition for dust particle size distribution scenario S3 (previous model, COCOSYS V2.4 beta)

It can thus be stated that the retention of dust in the confinement is almost solely based on the remaining of dust laden gas inside the building after pressure equalisation. For the other scenarios S1 and S2, deposition is slightly lower than for S3 - the minor differences do not necessitate additional figures. Any influence of particle size distribution on release behaviour is mainly due to differences in the remobilization from the primary circuit as shown in figure 10. Dust deposition in the confinement is generally low and mostly only takes place after a major part of release into the environment has already occurred.

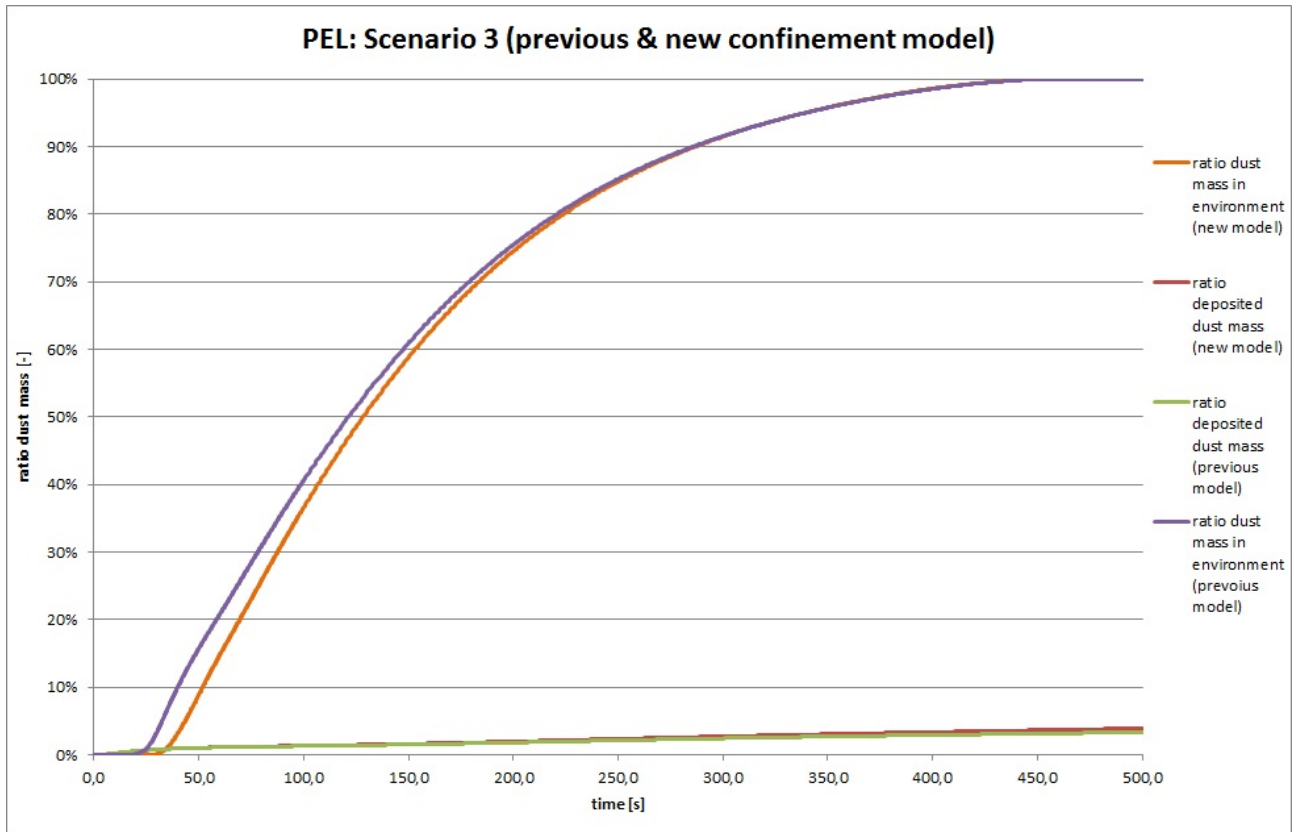


Figure 7-2: Relative dust release and deposition for dust particle size distribution scenario S3 (previous and new model)

Above Figure 7-2 shows the relative dust release and the ratio of deposited dust mass for both the previous and the refined grid of the new confinement nodalisation. The ratio of dust mass in the environment proceeds slower with the new nodalisation (dark orange curve) than with the previous nodalisation (dark violet). This slower progress in dust concentration is plausible, since COCOSYS is a zero-dimensional lumped-parameter code, which calculates uniform conditions within the gaseous phase of a cell. When increasing the number of cells, numerical induced diffusion reduces (the artificial enlargement of concentration gradients reduces) and so the reliability of simulation of local dust concentration improves. Nonetheless, the effect of nodalisation is minor. The main conclusion from previous simulations is that only a minority of dust is deposited (curves clash almost during whole simulated time), whereas the majority of dust remains airborne was confirmed.

The relative fraction of the mass ratio each dust particle size class is compared for the dust mass ratio produced during reactor operation, the ratio of the dust mass entering the confinement from the leak and the dust mass ratio eventually released into the environment for the scenarios S1 - S3 in Figure 7-3 to Figure 7-8. Since the objective is to analyse size distribution, no conclusions to the relations of the total dust masses involved must be drawn from this illustration. It has to be pointed out that both "release" values were obtained through integration over the whole depressurisation phase; additionally, there is a significant time dependence of the spectrum of the dust leaving the primary circuit.

It is important to acknowledge that the fractions shown in each figure describe a spectrum and not absolute values for the dust mass in a particle size class. E.g., the absolute released masses are several orders of magnitude lower than the production in any particle size class.

Generally, the influence of the confinement on the dust spectrum is marginal. The shift towards smaller particle diameters (compared to the dust originally produced in the reactor) occurs mainly in the primary circuit, as larger particles are more prone to deposition. The influence of containment phenomena on particle distribution is analogous, though even smaller. The fact that most of the dust mass relevant for environmental concern has a particle size between approx. $0.5 \mu\text{m}$ and $5 \mu\text{m}$, can serve as a first approach for potential solutions to retain dust.

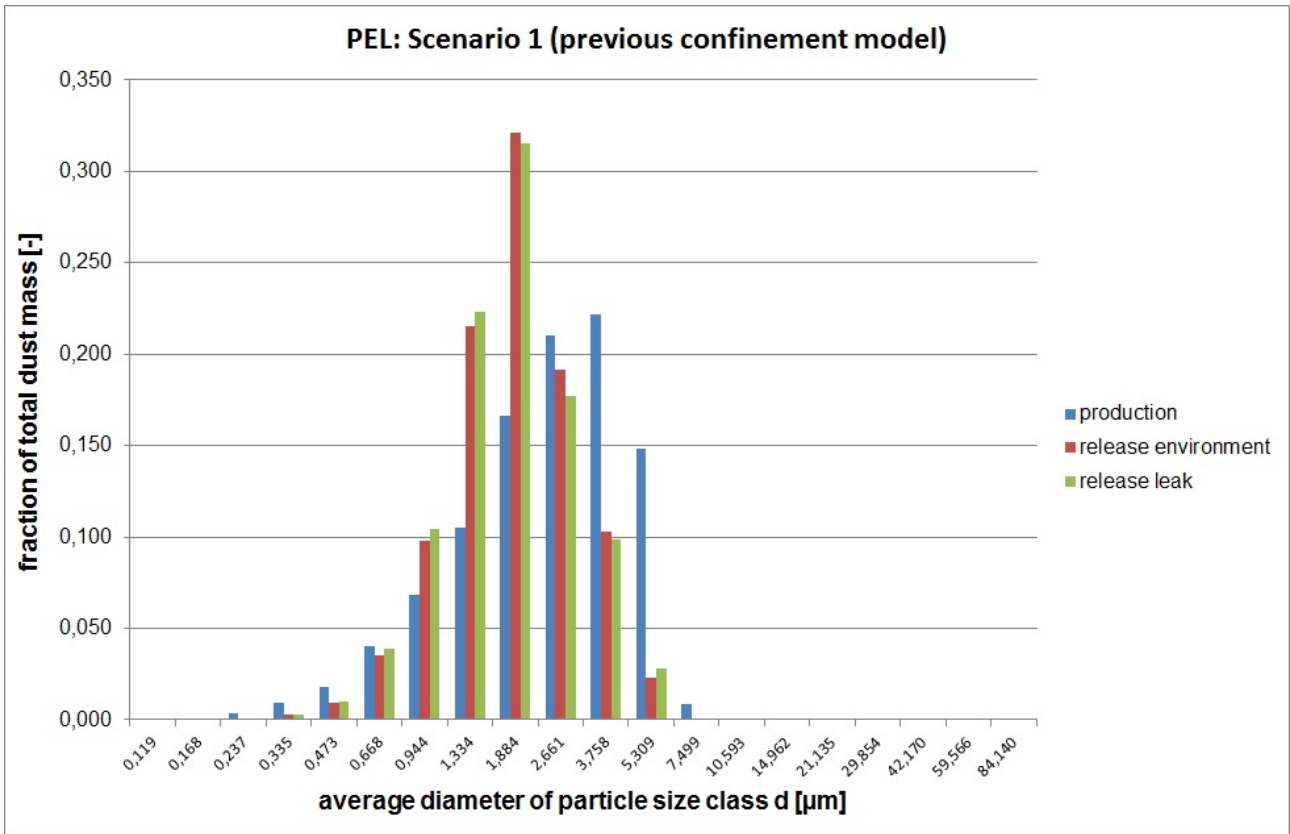


Figure 7-3: Dust spectrum comparison for scenario S1 (previous model, COCOSYS V2.4 beta)

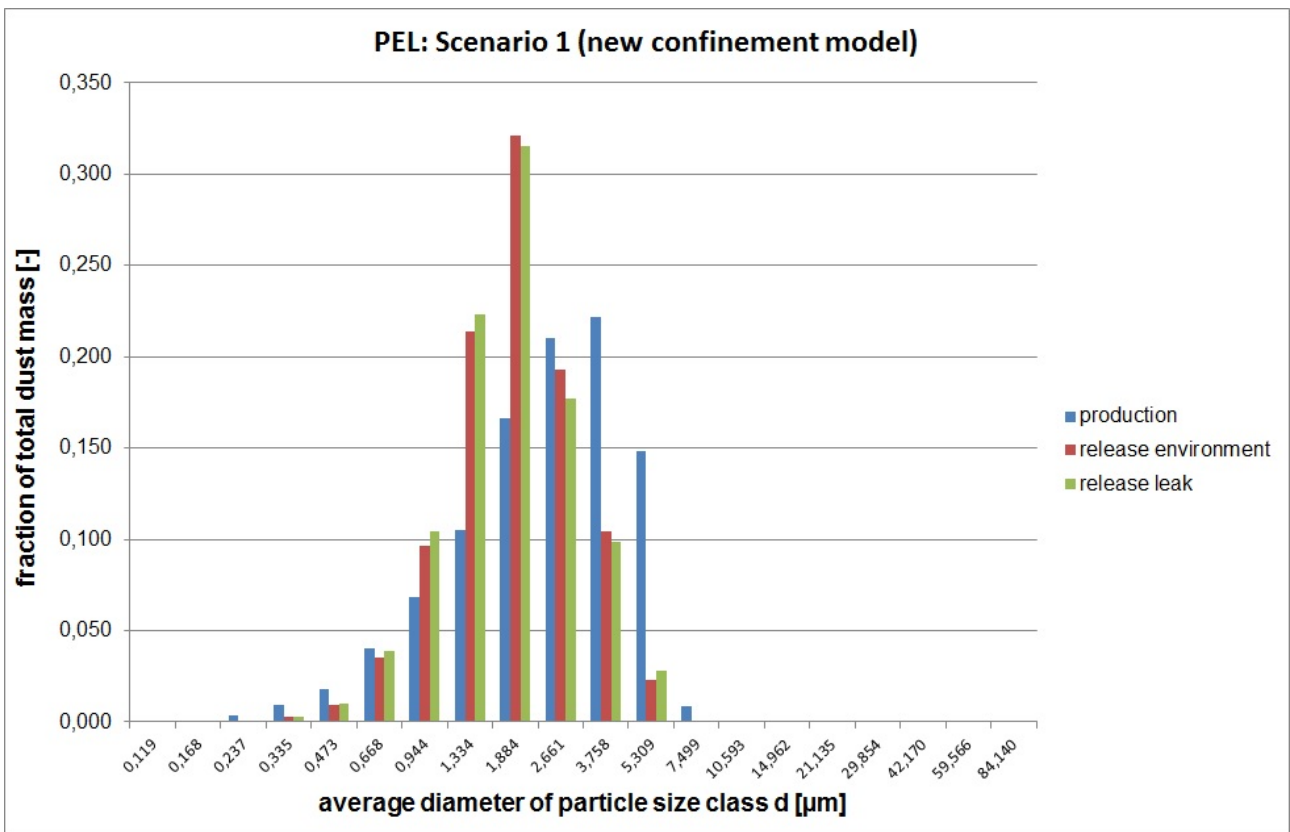


Figure 7-4: Dust spectrum comparison for scenario S1 (new model, COCOSYS V2.4)

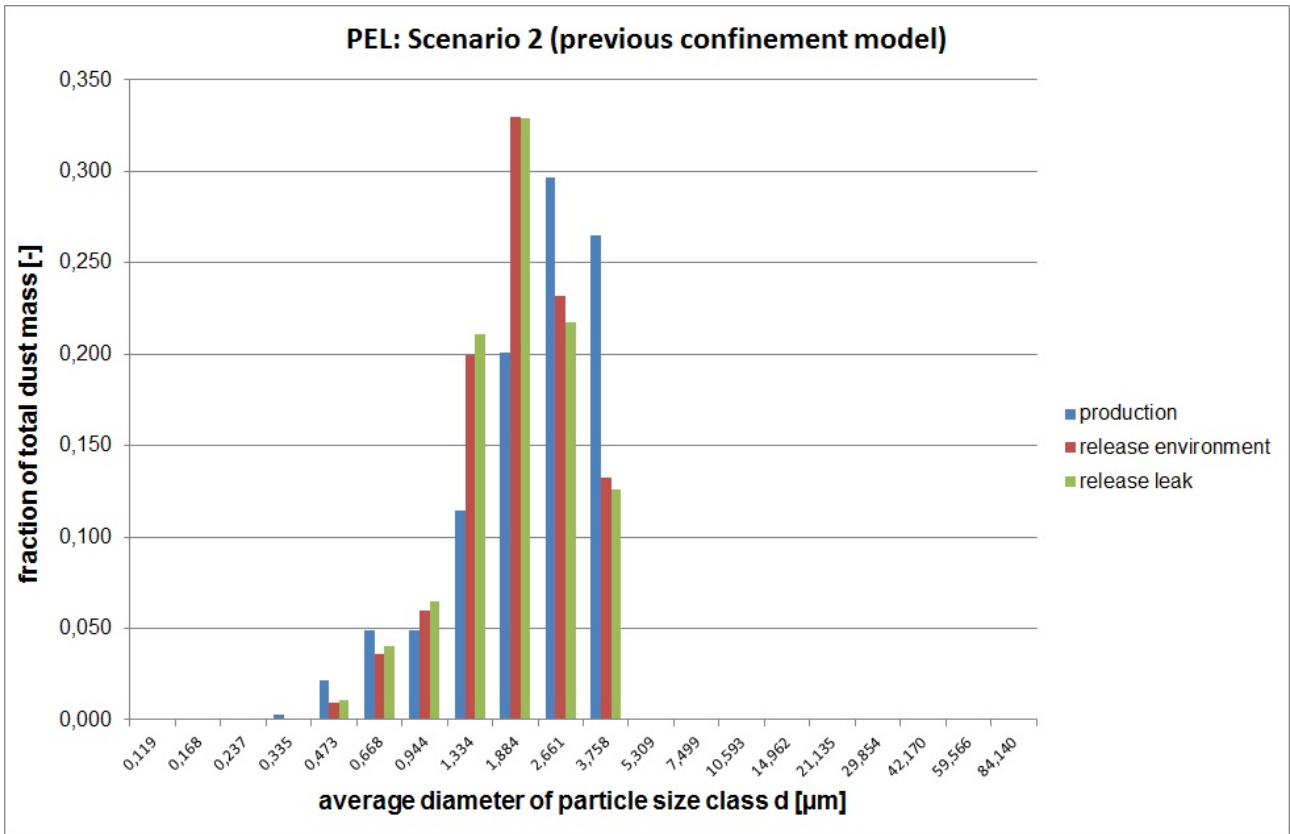


Figure 7-5: Dust spectrum comparison for scenario S2 (previous model, COCOSYS V2.4 beta)

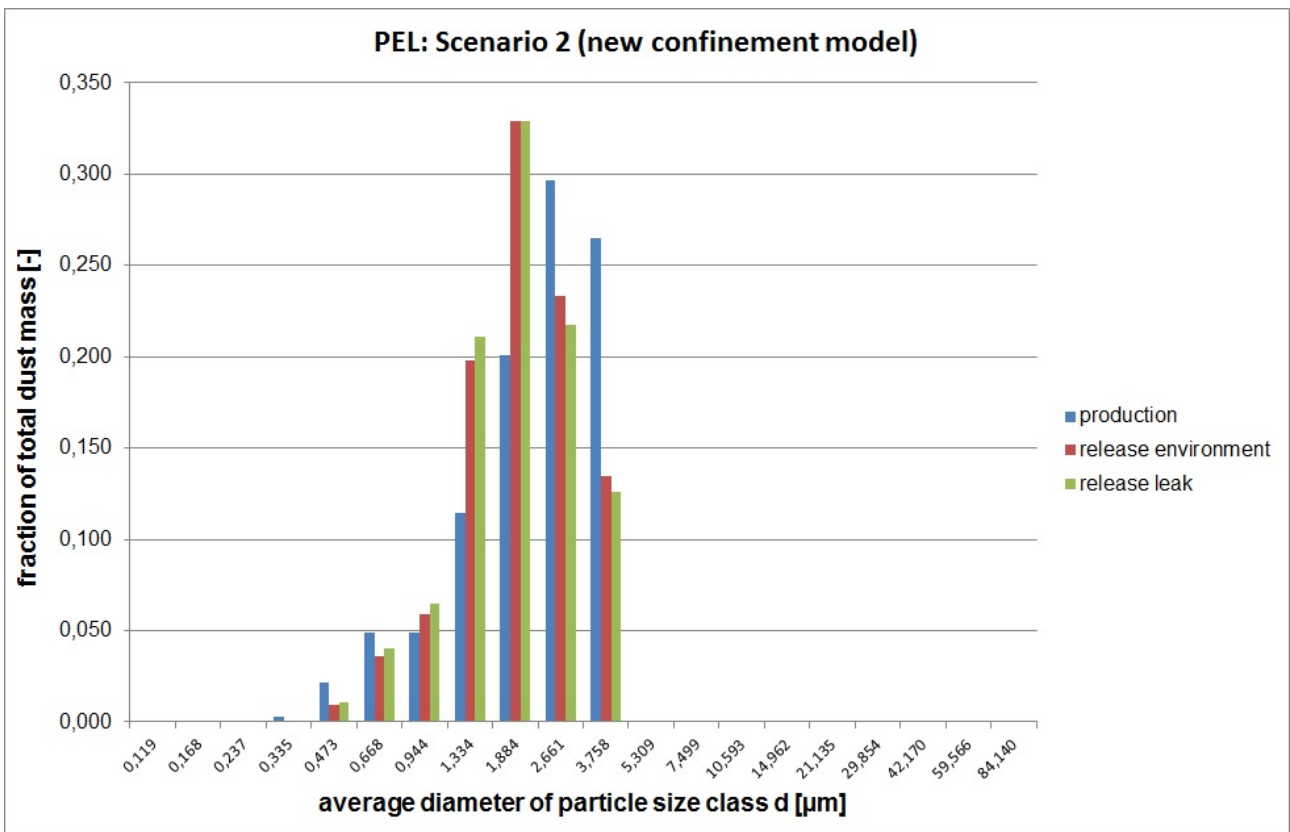


Figure 7-6: Dust spectrum comparison for scenario S2 (new model, COCOSYS V2.4)

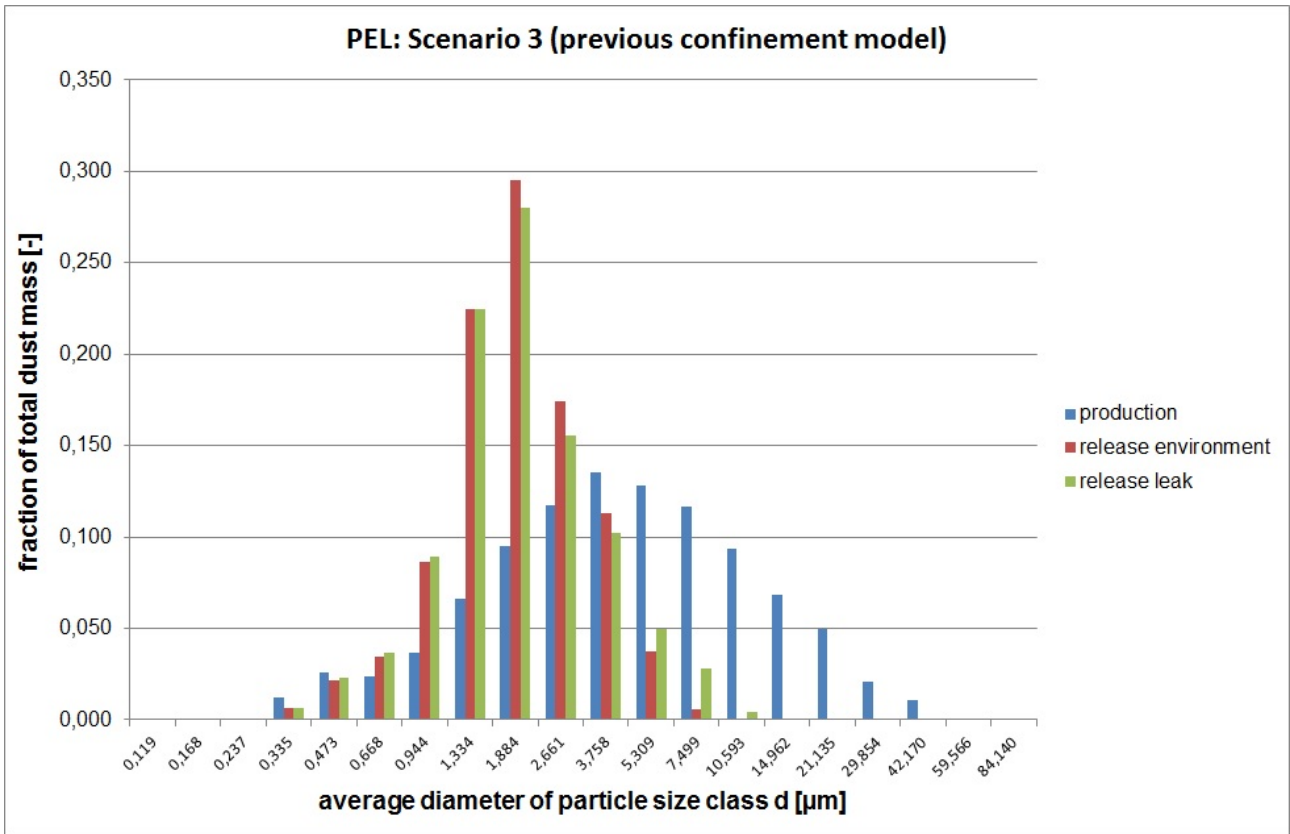


Figure 7-7: Dust spectrum comparison for scenario S3 (previous model, COCOSYS V2.4 beta)

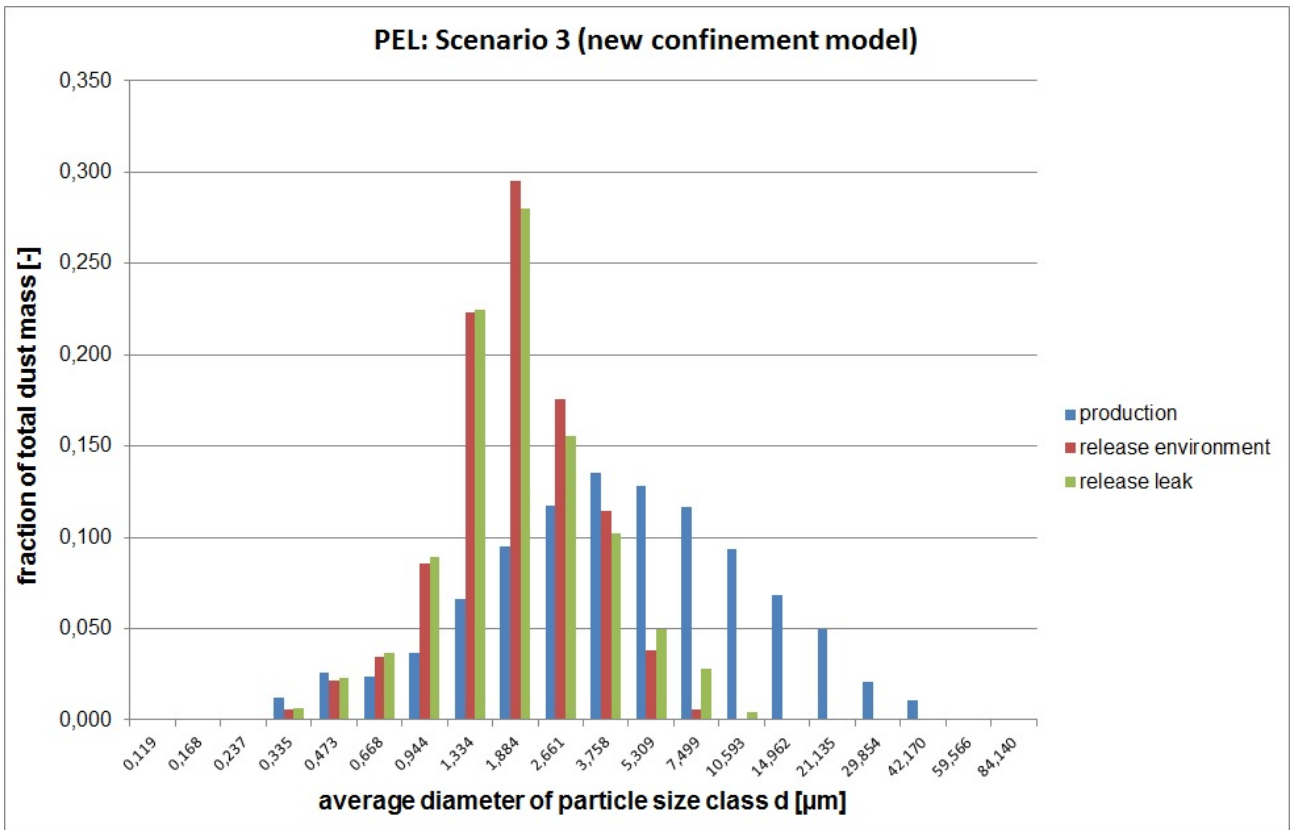


Figure 7-8: Dust spectrum comparison for scenario S3 (new model, COCOSYS V2.4)

7.2 Results for calculated dust behavior at FFE break

In this chapter the results for a break of pipe socket of the fuel feed line (FFE) are displayed. While the FFE itself is a DN 65 pipe, the break at the pipe socket results in a beyond design break at the bottom of the RPV with a diameter of 350 mm, which equals an outlet area of 962 cm².

Like PEL this scenario was simulated with the old as well as the new confinement nodalisation under use of both, COCOSYS V2.4 beta and COCOSYS V2.4. As results for PEL already demonstrate, only negligible differences can be found in results of both code versions. So in this chapter only results obtained with COCOSYS V2.4 are presented.

The effect of the confinement for dust retention calculated with the COCOSYS model and based on the gas and dust injection provided by the DIREKT/STAR simulation for the break of the fuel feed line and the expected case of dust adhesive force parameters is summarized in table 3.

Table 4: Confinement dust balance for dust particle size distribution scenarios S1 - S3 for FFE

	S1	S2	S3
Total dust mass injected into confinement	3 533 g	3 967 g	2 026 g
Total dust mass released into ENV	1 901 g	2 182 g	1 031 g
Released fraction	54 %	55 %	51 %

In general, the total as well as the relative amount of dust released into the confinement and in the end into the environment is much higher for FFE than for PEL. Consequently, above figures have to exceed dust release after PEL break by far, which is in line with Figure 4-1 to Figure 4-3, those vertical axes differ by three orders of magnitude.

The released fraction of the injected dust is generally higher for FFE than for PEL breaks. At the smaller PEL break (20 cm²), dust laden primary coolant enters the reactor building slowly, displacing the air originally present. Consequently, the gas exiting into the environment at the beginning of the pressure release has only low dust concentrations. For a larger break like the FFE scenario, the primary coolant enters the reactor building faster than gas can be released through the exhaust vent, leading to a significant pressure build-up and mixing with the air in the confinement before significant amounts of gas have left the building. Thus, the exhaust gasses contain a higher percentage of the dust injected right from the beginning of the accident phase.

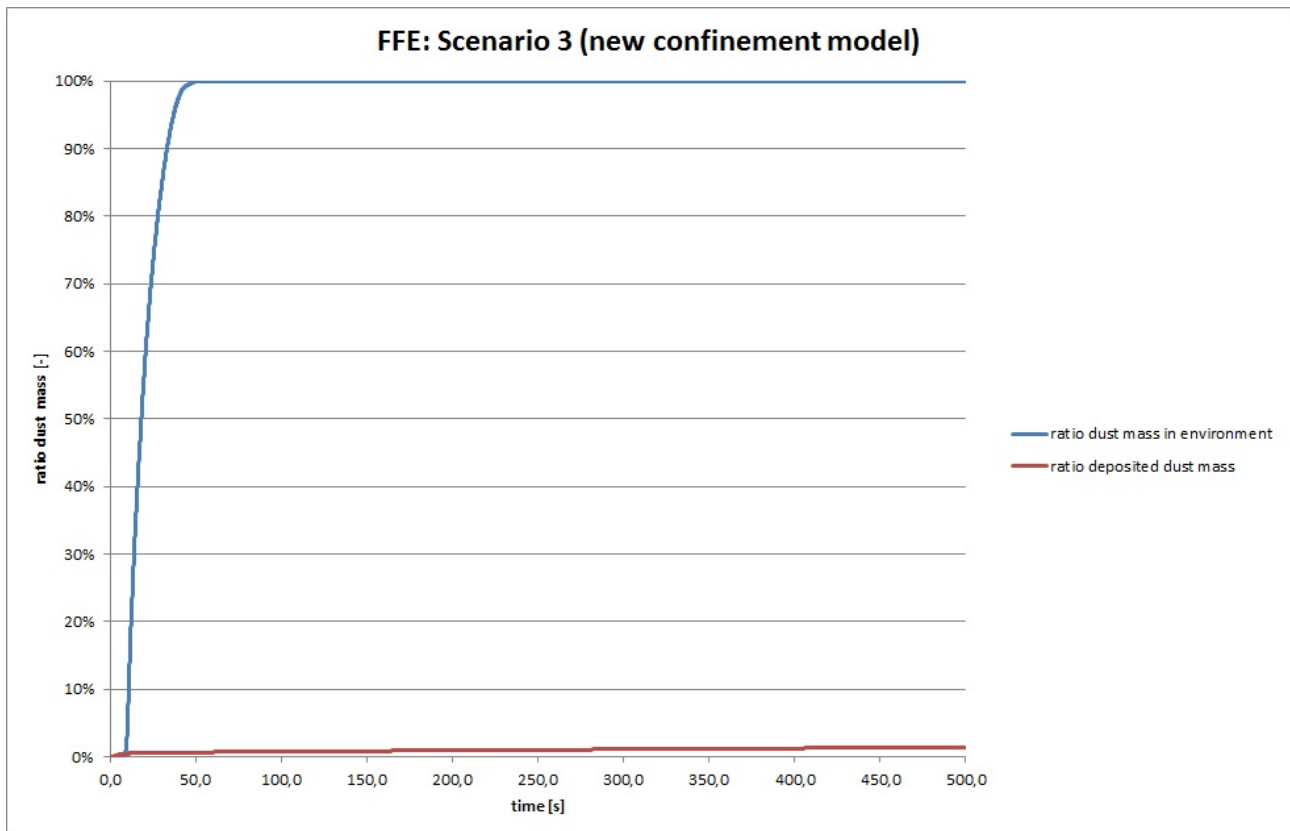


Figure 7-9: Relative dust release and deposition for dust particle size distribution scenario S3 (new model)

When comparing Figure 7-9: Relative dust release and deposition for dust particle size distribution scenario S3 (new model) to the corresponding diagram for PEL (Figure 7-1 on p. 23) it confirms the previous assumption that results for FFE might not differ too much from ones for PEL as right, but only regarding the ratios of deposited / released dust mass. In relation to release time all processes run much faster after a FFE break, so that the complete release occurs in less than a minute after the break. This is reasonable, since for a larger break the pressure equalisation takes significantly less time.

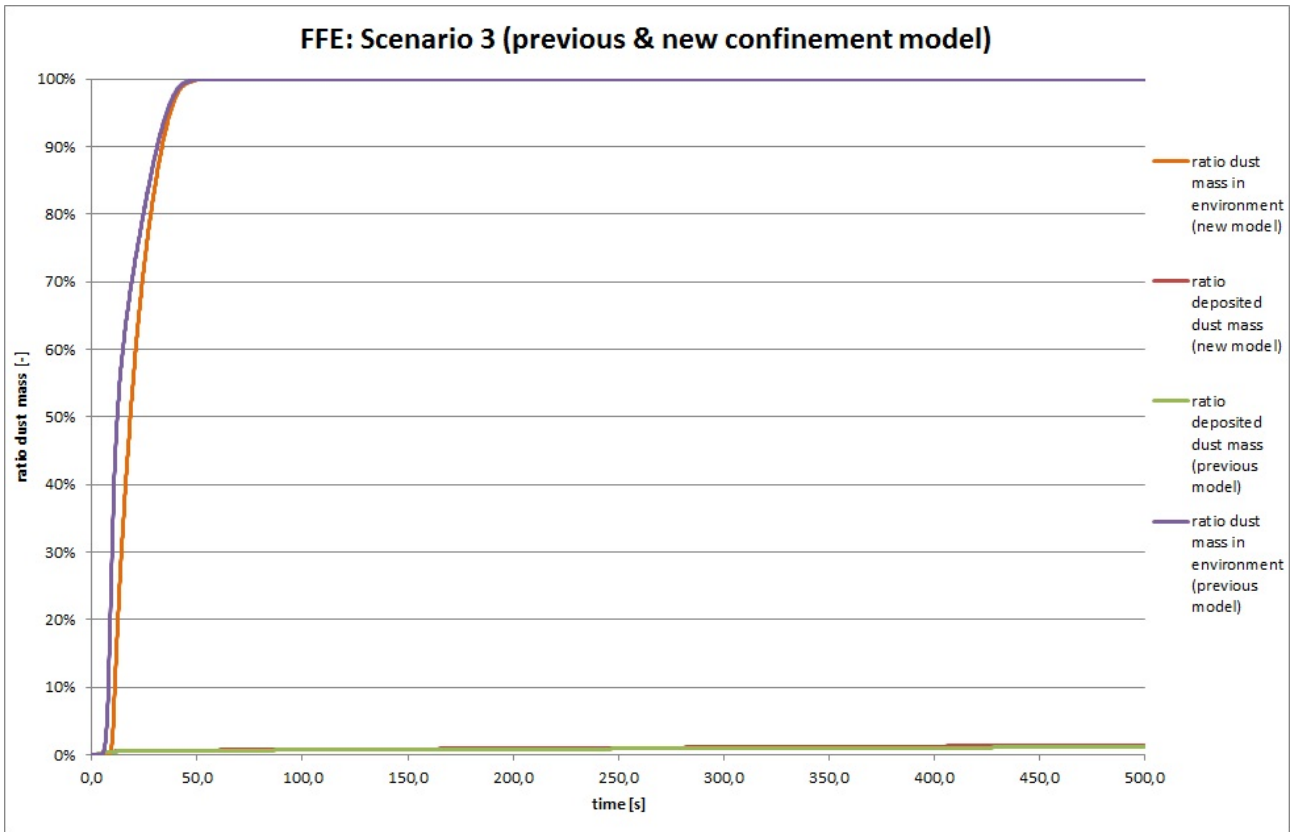


Figure 7-10: Relative dust release and deposition for dust particle size distribution scenario S3 (previous and new model)

The comparison of dust ratio progress between the previous and the new nodalisation of the confinement indicates the same as in Figure 7-2: release ratio in the environment increases slightly slower for the new confinement model, due to improved numerical induced diffusion, but the deviations are quite small.

In the following figures (Figure 7-11 to Figure 7-13) the relative fraction of each dust particle size class for the scenarios S1 - S3 is displayed. As already discussed, those values are integral values over the whole simulation time and do not considerate time-dependency of the release any more.

Again, the relative fractions refer to three different cases: dust production during reactor operation time, dust entering the confinement via the leak and the dust eventually released into the environment.

Like for the PEL break, It is important to acknowledge that the fractions shown in each figure describe a spectrum and not absolute values for the dust mass in a particle size class. E.g. the absolute released masses are several orders of magnitude lower than the production in any particle size class.

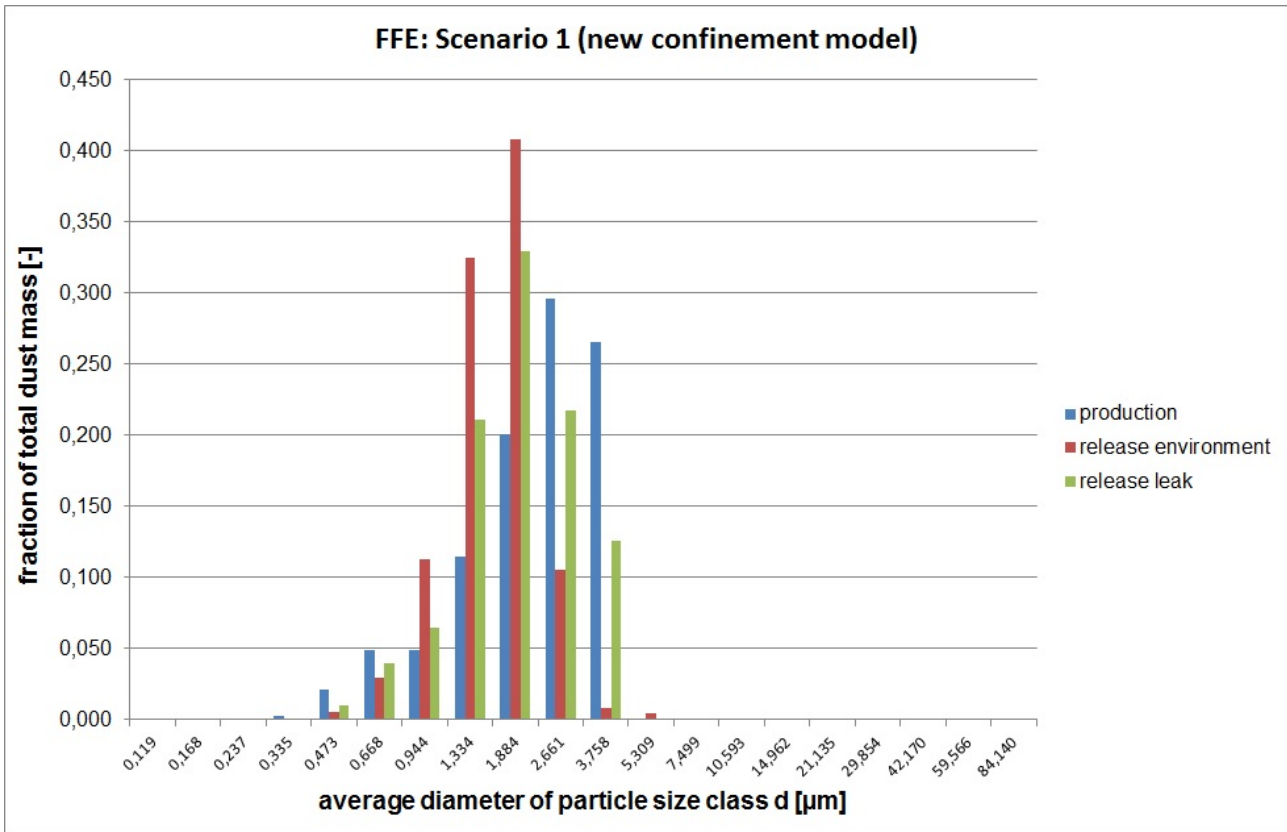


Figure 7-11: Dust spectrum comparison for scenario S1 after FFE break

The observable trend – like for PEL break – to a higher proportion of smaller particle diameters (compared to the dust originally produced in the reactor) is mainly due to the corresponding injection rates. Due to above illustrations, the majority of the potentially released dust mass has particle diameters between approx. 0.5 µm and 5 µm. Within these size classes, special focus has to be cast on particles between 1.0 µm and 2.0 µm: while for PEL approx. 50 - 60 % of all into the environment released mass that has particles sizes, the procedure is for FFE with ca. 75 % even stronger. When interpreting the results for dust spectrum, one needs to consider that the ratio in all diagrams is a mass ratio, not particle number ratio. When analysing the number of particles per class, the majority of particles can be found in size classes below 1 µm, compare e.g. Figure 4-1 on p.11.

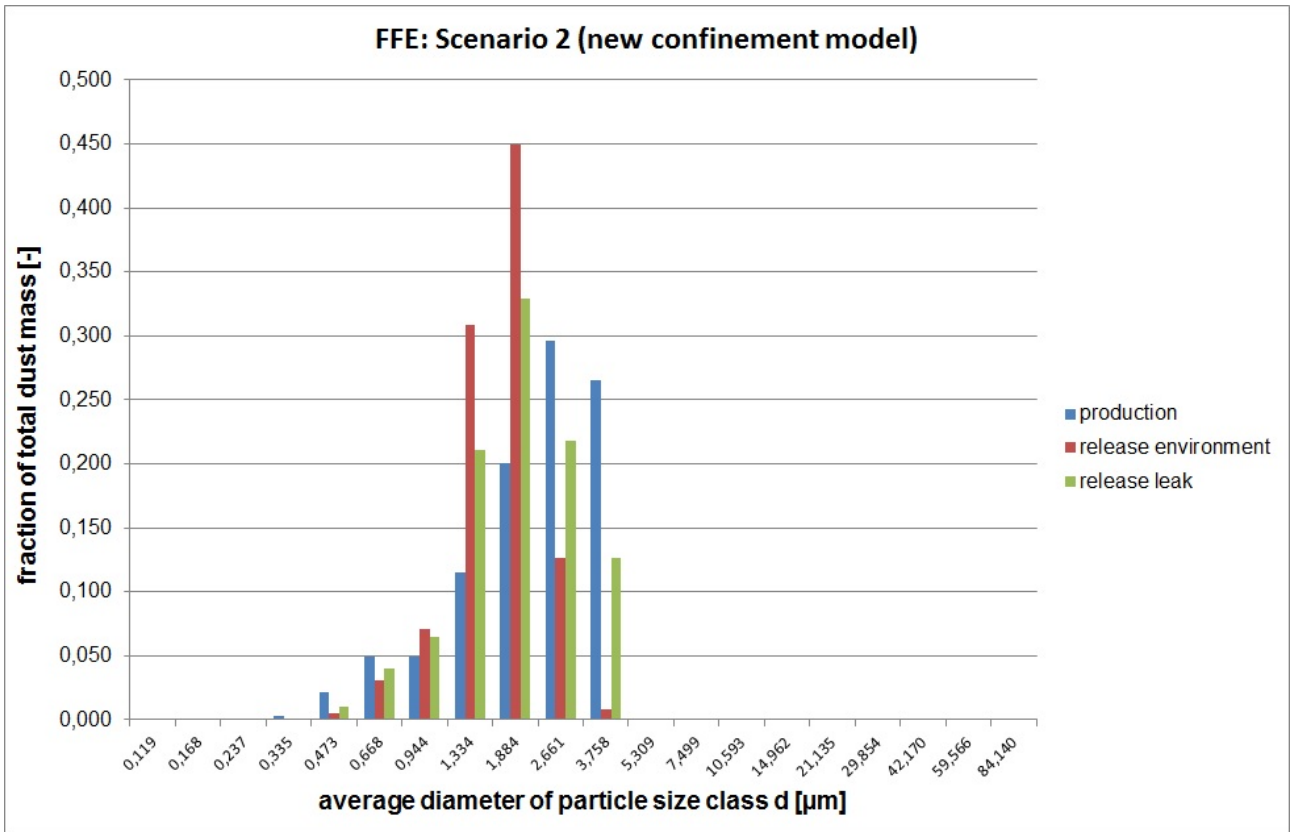


Figure 7-12: Dust spectrum comparison for scenario S2 after FFE break

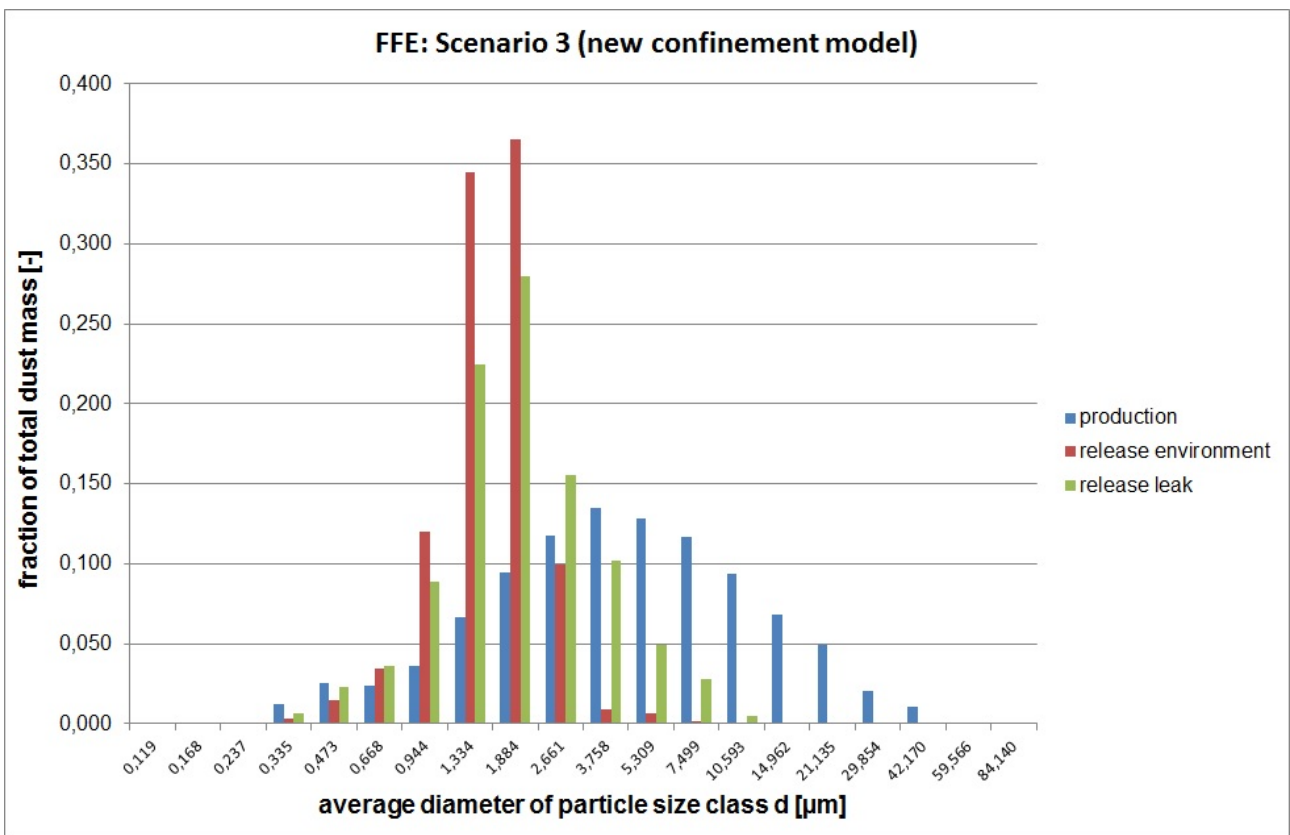


Figure 7-13: Dust spectrum comparison for scenario S3 after FFE break

8 Potential consequences of COCOSYS' limitations

Like every code used for simulation of physical phenomena, COCOSYS has limitations. In this chapter, these limitations are examined and its potential influence about simulation results are evaluated.

8.1 Turbulent deposition

Turbulent deposition is a generic term for several mechanisms carrying particles through the vicious sublayer of a turbulent flow, most notably diffusion and eddy impaction [HIN99].

Currently, no model for turbulent deposition is implemented in COCOSYS. A simple correlation for deposition velocity is given by [WOO81], for which [AHM97] confirms a good match with experimental results.

$$v_{dep,turb} = u_{\tau} \cdot \left(0,057 \cdot Sc^{-\frac{2}{3}} + 4,5 \cdot 10^{-4} \cdot \tau^{+2} \right)$$

Here, u_{τ} is the friction velocity, Sc the Schmidt-number of the particles and τ^{+} the dimensionless relaxation time, which is derived from the particle relaxation time τ according to the following equation:

$$\tau^{+} = \tau \cdot \frac{u_{\tau}^2 \cdot \rho_{fl}}{\eta}$$

In order to evaluate the importance of this mechanism, the pressure relief shaft was selected as a reference volume and evaluated for the PEL break. Deposition as modelled with COCOSYS and integrated mass flow through the zone were taken from the calculation results; additionally, turbulent deposition was calculated with the correlation stated above and converted into deposited mass according to [HIN99].

The results are presented in Table 5 for PEL and for FFE in Table 6:

Table 5: Comparison of effects of implemented deposition models, turbulent deposition and integrated dust mass flow for PEL

	S1	S2	S3
Total dust mass deposited according to implemented models (all deposition phenomena)	$1.0 \cdot 10^{-5} \text{ g}$	$1.1 \cdot 10^{-5} \text{ g}$	$6.6 \cdot 10^{-6} \text{ g}$
Total dust mass deposited due to turbulent deposition (manual calculation according to [Hin99])	$5.5 \cdot 10^{-2} \text{ g}$	$6.6 \cdot 10^{-2} \text{ g}$	$3.5 \cdot 10^{-2}$
Integrated dust mass flow	9.3 g	11.0 g	5.7 g

Table 6: Comparison of effects of implemented deposition models, turbulent deposition and integrated dust mass flow for FFE

	S1	S2	S3
Total dust mass deposited according to implemented models (all deposition phenomena)	$2.05 \cdot 10^{-1} \text{ g}$	$2.23 \cdot 10^{-1} \text{ g}$	$1.20 \cdot 10^{-1} \text{ g}$
Total dust mass deposited due to turbulent deposition (manual calculation according to [Hin99])	18.6 g	21.1 g	10.6 g
Integrated dust mass flow	3 125 g	3 565 g	1 728 g

As indicated by the tables above, dust masses on the surfaces due to turbulent deposition via manual calculation are three orders of magnitude higher than the ones due to all deposition models implemented in COCOSYS so far. Thus, a deposition mechanism with a high relevance for depressurisation accidents of HTR is so far missing in this code system. A further check in the Reference Manual of the implemented models in COCOSYS reveals that all potential deposition processes (sedimentation, diffusion,

thermophoresis, diffusiophoresis) neglect the influence of the flow velocity. The consultation with the developers confirmed that implemented models are currently only reliable for small flow velocities. During depressurisation accidents the pressure relief shaft is a zone with high gas velocities which favour turbulent deposition. So the difference between the particular dust masses deposited due to turbulent deposition or due to implemented models can be expected to be significantly lower in other zones. Furthermore, a comparison of turbulent deposition to the integrated dust mass flow makes clear that dust is predominantly not deposited and remains gas borne. Consequently, the results for released dust masses presented in Table 3 and Table 4 are not expected to change much upon integration of turbulent deposition into COCOSYS. Nonetheless, in order to generally qualify the code system for the simulation of HTR depressurisation accidents, this would be a worthwhile addition.

8.2 Resuspension

The only way to simulate resuspension in COCOSYS so far is via the Fromentin model based upon the work of [FRO89], [NOW08]. However, the goal of this implementation was to simulate the effect of pressure transients (e.g. from a hydrogen deflagration) on a pre-defined particle layer. [KLE10] Especially for a simulation of the interaction of deposition and resuspension, this approach is not suitable. An alternative would be the quasi-static Rock'n Roll model, which is also implemented in the STAR code as well as other severe accident codes like ASTEC [BUJ10].

For the cases simulated here, both PEL and FFE, modelling resuspension of dust deposited on confinement walls will not significantly increase the dust source term because deposition is already very low. In case of FFE, dust deposition is even once more lower than for PEL, since the FFE scenario processes faster than the PEL. For other accident scenarios the effect might be more interesting, especially since the non-consideration of resuspension is intrinsically non-conservative. However, it must be emphasized that the challenge of identifying suitable particle adhesive force parameters faced for the STAR-simulation will also be faced for the containment code if resuspension is implemented.

8.3 Variability of atmospheric material values

So far, not all material values calculated in THY were actually available for the AFP calculation. For example, the molecular weight of the gas mixture and its thermal conductivity (actually, that value divided by the thermal conductivity of the particle) are to be entered by the user and remain constant during the whole simulation rather than using values from THY. Since deposition was shown to be a minor issue and in fact, each aerosol particle class acted mostly like an inert, additional gas component, simply following the fluid without major interactions, these changes are not vital for improving the predictability of the dust source term of HTR depressurisation accidents.

Like other potential improvements to be discussed below, this constitutes a major modification of the COCOSYS code, which can only be performed by its official developers at GRS.

8.4 Characteristic lengths for simulation of thermophoresis

In COCOSYS, the aerosol model uses a characteristic length of 3 mm as constant boundary layer thickness to calculate the temperature gradient for thermophoresis. It would be a significant improvement to replace that constant value with a simple calculation based upon the theory of heat transfer and applied e.g. by [STE10] and [JÜH11].

By equalising the heat flux for the boundary layer and the heat transfer from fluid to wall, the following expression for the temperature gradient is obtained:

$$\dot{q}'' = \lambda_{fl} \cdot \nabla T$$

$$\dot{q}'' = \alpha \cdot (T_w - T_{fl})$$

$$\Leftrightarrow \nabla T = \frac{\alpha}{\lambda_{fl}} \cdot (T_w - T_{fl})$$

The heat transfer coefficient α can be made available from the respective calculation in THY. However, an implementation into COCOSYS' source code would require substantial validation efforts. Additionally, one has to keep in mind when working on correlations for boundary layers in COCOSYS' source code that changes must be valid for all accident scenarios; and even more important, changes have to be valid not only for dust deposition in HTR, but also aerosol deposition in light water reactors. The necessary capacity for this sort of code development can only be provided by COCOSYS' developer – GRS – itself. Regarding the results of Chapter 7 the static definition of thermophoresis' boundary layer has very little impact, since the majority of dust is not deposited at all.

8.5 Input structure of injection tables

The existing input structure of COCOSYS is clearly focused on injecting aerosol with a mathematically described (generally lognormal) particle size distribution. Creating injection tables for irregular, time-dependent size distributions is only possible with a disproportionate effort and by no means through simply including external files.

Thus, simple improvements in the input routines could make the integration of aerosol injection data generated by primary circuit codes much easier and so less error-prone, especially facilitating calculations with parameter variations.

Like other COCOSYS improvements presented in this deliverable, this issue can only serve as a proposal for further development of the code package, particularly since the improvement only has an impact on user-friendliness, but not on the quality of the calculation of HTR-dust behaviour.

9 Summary and Perspective

The blow-down phase of a depressurisation accident of an HTR has been simulated with COCOSYS. For the reference plant HTR-Module 200, the dust mass released into the environment has been calculated based upon a detailed modelling of the primary circuit which is not covered by this deliverable. As representative accident scenarios a break of the Pressure Equalization Line (PEL) as a design basis accident and a break of the pipe socket of the Fuel Feed Line (FFE) as beyond design basis accidents are analysed within a COCOSYS modelling of the confinement.

Based on the calculations performed, it can be stated that depending on the leak location about half up to two thirds of the dust released from the primary circuit are retained within the confinement. Reduction of dust source term is almost exclusively due to dust laden gas which remains in the building after pressure equalisation while dust deposition is insignificant.

As dust spectrum comparisons indicate, there is no major change from particle size distribution of the originally present dust, neither due to resuspension and transport in the primary circuit nor by phenomena in the reactor building. Instead the results are dominated by the presumed particle size distribution of Table 1.

Turbulent deposition and dry resuspension have been identified as relevant mechanisms that are not covered by suitable COCOSYS models yet. Their influence has been tentatively evaluated and found to be not decisive for the dust source term, see Chapter 8. So the points for improvement mentioned in previous chapters are not to be expected to have significant influence on the results. However, their inclusion into COCOSYS will contribute to reinforce its significance as a best-estimate code system as well as to improve the code's capability and reliability when simulating other scenarios, whose resulting source terms strongly depend on above phenomena.

As a final conclusion from performed simulations it can be stated that COCOSYS V2.4 is capable to reliably determine a dust source term after a depressurisation accidents in HTRs. Like demonstrated, the changes from COCOSYS' beta version to the released version have hardly any relevance for the phenomena analysed for this deliverable. The simulations with a finer nodalisation of the containment generally show a similar dust behaviour and confirm previous results.

The general validation and especially a proper verification of COCOSYS is going to take a considerable amount of time as well as – if situation should arise – to modify the physical models implemented in COCOSYS. During the term of the ARCHER project potential for improvements can be identified and reported to COCOSYS developers, but an improved COCOSYS code will unfortunately not be available. Nonetheless, simulations with an improved code might be a yielding item in future research projects.

As the predictive quality of the COCOSYS calculation was shown to be quite good, the focus shifts to other elements of the source term chain that have much higher uncertainties:

- The selection of appropriate parameters characterizing the adhesion and thus the resuspension of dust can impact the source term by more than an order of magnitude and is still subject to ongoing research, most notably the TARGET²-project. The experiments are conducted at the Forschungszentrum Jülich and experimental data are presumed to be available by the end of this year. This might be a great opportunity to validate the current calculations on reliable experimental data.
- Furthermore, to evaluate the COCOSYS results, one has to draw conclusions from the released dust mass to the released radioactivity. Assumptions about this correlation have been made in [INT561] and [JÜH11], but the problem is again the uncertainty of the results. There have already been made educated guesses about the amount and the spectrum of dust produced in the HTR as well as the release in the confinement respectively the environment. Now adding the uncertainties from the correlation between dust mass and radioactivity will further increase the error range. The work of [XHO] shows a promising perspective of improving the quality of the calculated fission product source term.

² Transport, Ablagerung und Resuspension graphitischen Staubs in Heliumatmosphäre bei hohen Temperaturen (English: Transport, Deposition and Resuspension of graphitic dust in a helium atmosphere under high temperatures)

Due to the limited scope of the work within this deliverable as well as the above mentioned issues for future research, no general prescription for additional protective measures (like filtered venting or a pressure tight containment) can be given. However, it was shown that COCOSYS is a valuable and reliable tool for analysing a central aspect of the source term chain of HTR depressurisation accidents.

10 Literature

- [AHM97] Ahmadi G., Chen Q.: *Deposition of particles in a turbulent pipe flow*, Journal of Aerosol Science, Vol. 28 Nr. 5, p. 789-796, 1997.
- [AHM98] Ahmadi G., He C.: *Particle Deposition with Thermophoresis in Laminar and Turbulent Duct Flows*, Aerosol Science and Technology 29, p.525-546, 1998.
- [ALL08] Allelein H.-J. et al.: *COCOSYS: Status of development and validation of the German containment code system*, Nuclear Engineering and Design 238, p. 872-889, 2008.
- [BRO13] Broxtermann P., *Simulation passiver Kühlsysteme für Sicherheitsbehälter*, dissertation, RWTH Aachen 2013
- [BUJ10] Bujan A. et al.: *ASTEC V1.3 code SOPHAEROS module validation using the STORM experiments*, Progress in Nuclear Energy 52, p. 777-788, 2010.
- [BUR13] Burkhardt, J., *Analyse, Simulation und Modellierung der Erosion atmosphärischer Schichtungen mit Lumped Parameter-Codes*, dissertation, Ruhr-Universität Bochum, 2013
- [CAR05] Carpick R.W., Grierson D.S., Flater E.E.: *Accounting for the JKR–DMT transition in adhesion and friction measurements with atomic force microscopy*, Journal of Adhesion Science and Technology, Vol. 19, Nr.3-5, p. 291-311, 2005.
- [ERD91] Erdmann W.: *Unterteilung von Strukturen in Temperaturnodes (Layer) zur Simulation mit der instationären 1 D-Wärmeleitgleichung (Programm WAND)*, Technical Note, GRS Köln, 1991.
- [FAC08a] Fachinger J. et al.: *Examination of Dust in AVR Pipe Components*, Proceedings of the 4th International Topical Meeting on High Temperature Reactor Technology (HTR2008), Washington DC, USA, 28. September – 1.October 2008.
- [FAC08b] Fachinger J. et al.: *Auswerteprotokolle zum Projekt „Dust Experiments on AVR Components“ (DEACO)*, 2008.
- [FON09] Fontanet J. et al.: *Modelling of HTR Confinement Behavior during Accidents Involving Breach of the Helium Pressure Boundary*, Science and Technology of Nuclear Installations, Article ID 687634, Volume 2009, 2009.
- [FRO89] Fromentin A. : *Particle Resuspension from a Multi-Layer Deposit by Turbulent Flow*, Programm LWR-Sicherheit, Paul Scherer-Institut, PSI Bericht 38, Villingen 1989.
- [GOR82] Goren S. L., D'Ottavio T.: *Aerosol Capture in Granular Beds in the Impaction Dominated Regime*, Aerosol Science and Technology 2, p. 91-108, 1982.
- [GOT90] Gottaut H., Krüger K.: *Results of experiments at the AVR Reactor*, Nuclear Engineering and Design 121, p. 143-153, 1990.
- [HER07] Herranz L. E., Del Prá C.L.: *Major challenges to modeling aerosol retention near a tube breach during steam generator tube rupture sequences*, Nuclear Technology, Vol. 158, p. 83-93, 2007.
- [HIN99] Hinds C. W.: *Aerosol Technology – Properties, Behavior and Measurement of Airborne Particles*, John Wiley & Sons, Inc., 1999.
- [IAE97] *Fuel performance and fission product behavior in gas cooled reactors*, IAEA-TECDOC-978, 1997.
- [ING81] Ingham D.B.: *The diffusional deposition of aerosols in fibrous filters*, Journal of Aerosol Science, Vol. 12 Nr.4, p. 357-365, 1981.

- [INL11a] Pebble Bed Reactor Scoping Safety Study, Technical Data Record Document No.: 12 – 9149863 – 000, AREVA NP, available at:
https://inlportal.inl.gov/portal/server.pt/document/78533/pebble_bed_reactor_scoping_safety_study_-_areva_pdf
- [INL11b] Pebble Bed Reactor Plant Design Description, Technical Data Record Document No.: 12 – 9149697 – 000, AREVA NP, available at:
https://inlportal.inl.gov/portal/server.pt/document/78521/pebble_bed_reactor_plant_design_description_-_areva_pdf
- [INT560] *Aktivitätsfreisetzung und Strahlenexposition bei der HTR-Modul-Kraftwerksanlage – Teil I: Bestimmungsgemäßer Betrieb*, Technische Unterlagen für Gutachtergespräche, Ident-Nr. :76.00560.2, Interatom, 1987.
- [INT561] *Aktivitätsfreisetzung und Strahlenexposition bei der HTR-Modul-Kraftwerksanlage – Teil II: Störfälle*, Technische Unterlagen für Gutachtergespräche, Ident-Nr. :76.00560.2, Interatom, 1988.
- [INT679] *Belastungen des Reaktorgebäudes nach Rohrleitungsbrüchen*, Technische Unterlage entsprechend Unterlagenforderung, Ident-Nr. :76.00679.*, Interatom, 1988.
- [JÜH11] Jühe S.: *Kohlenstoffstaubfreisetzung bei Druckentlastungsereignissen von Hochtemperaturreaktoren*, Dissertation, RWTH Aachen, 2011.
- [JÜH12] Jühe S., Struth S., Schlögl B., Allelein H.-J.: *Simulation of Dust Behavior in HTR with Pebble Bed Fuel*, in: Proceedings TOPSAFE 2012.
- [JÜH12a] Jühe S., *Modelling of dust behavior in HTR confinements during depressurisation accidents with COCOSYS*, ARCHER deliverable D23.61 – revision 1, 2012
- [KLE10] Klein-Heßling W. et al.: *COCOSYS V2.4 User's Manual*, Gesellschaft für Anlagen- und Reaktorsicherheit, Köln, 2010.
- [LÖF88] Löffler F.: *Staubabscheiden*, Thieme Verlag, Stuttgart, 1988.
- [NOW08] Nowack H.: *Aerosolverhalten im Sicherheitsbehälter beim Einsatz von Rekombinatoren und nach Wasserstoffverbrennungen*, Dissertation, Bochum, 2008.
- [OET89] Oetjen H.-F.: *Arbeitsprotokoll zu Behandlung der Proben und Bestimmung von Kornspektren an den THTR-Staubproben*, AP-6-89, Forschungszentrum Jülich, 1989.
- [REE01] Reeks M. W., Hall D.: *Kinetic models for particle resuspension in turbulent flows: theory and measurement*, Journal of Aerosol Science 32, S. 1-31, 2001.
- [REU84] Reutler H., Lohnert G.H.: *Advantages of going modular in HTRs*, Nuclear Engineering and Design 78, p. 129-136, 1984.
- [SCE88] Scheibel H. G. et al.: *Untersuchungen der Spaltprodukt-Rückhaltung durch HTR-Reaktorschutzgebäude nach dem Vented-Confinement-Konzept*, Abschlussbericht BF-R-40.039-1.0, Battelle-Institut e.V. Frankfurt, 1988.
- [STE10a] Stempniewicz M. M., Winters L., Caspersson S. A.: *Analysis of Dust and Fission Products in a Pebble Bed NGNP*, Proceedings of the 5th International Topical Meeting on High Temperature Reactor Technology (HTR2010), Prague, 18.-20. October 2010.
- [STE10b] Stempniewicz M. M.: *SPECTRA – Computer Code Manuals*, NRG, Arnhem, 2010.
- [STE82] Stelzer J. F.: *Die Lösung der stationären und instationären Temperaturfeldgleichung*, Seminar Notes, Essen, 1982.
- [TAL80] Talbot L. et al.: *Thermophoresis of particles in a heated boundary layer*, Journal of Fluid Mechanics 101, p. 737-758, 1980.
- [WOO81] Wood N.B.: *A simple Method for the calculation of turbulent deposition to smooth and rough surfaces*, Journal of Aerosol Science, Vol. 12 Nr. 3, p. 275-290, 1981.

11 Annexes

Annex 1 – Document approval by beneficiaries' internal QA

11.1 Annex 1: Document approval by beneficiaries' internal QA

Fill involved beneficiaries as appropriate (mandatory for Milestones and Deliverables, but optional for other document type)

#	Name of beneficiary	Approved by	Function	Date
1	RWTH Aachen – LRST	D. Singh	Scientific Assistant	18/09/14
2	RWTH Aachen – LRST	Univ.-Prof. Dr. rer. nat. H.-J. Allelein	Head of Institute	18/09/14
3				
4				
6				
7				
8				
9				
10				
11				
12				
13				
14				
15				
16				
17				
18				
19				
20				
21				
22				